

**ASSESSMENT OF ATMOSPHERIC AEROSOL CONTENT IN ABUESI: A  
SUBURBAN COASTAL COMMUNITY IN GHANA**

BY

EMMANUEL BEMPONG-MANFUL

(10362529)

**(BSc. Physics, University of Cape Coast, 2010)**


THIS THESIS IS SUBMITTED TO THE UNIVERSITY OF GHANA, LEGON IN  
PARTIAL FULFILMENT OF THE REQUIREMENT FOR THE AWARD OF MPhil  
APPLIED NUCLEAR PHYSICS DEGREE

JULY, 2013.

## DECLARATION

This thesis is the result of research work undertaken by Emmanuel Bempong-Manful in the Department of Nuclear Sciences and Applications, Graduate School of Nuclear and Allied Sciences, University of Ghana, under the supervision of Dr. G. K. Banini and Prof. S. B. Dampare.

.....	.....
Emmanuel Bempong-Manful (Student)	Date
.....	.....
Dr. G. K. Banini (Principal Supervisor)	Date
.....	.....
Prof. S. B. Dampare (Co-Supervisor)	Date

The watermark is the official crest of the University of Ghana. It features a shield with a blue background and a yellow border. The shield is divided into three sections: the top section contains three yellow leaves, the middle section contains a yellow cross with four curved ends, and the bottom section contains a yellow banner with the Latin motto 'INTEGRI PROCEDAMUS'. The crest is centered on the page and serves as a background for the signature lines.

## DEDICATION

This research work is whole-heartedly dedicated to the memory of my late father, my family for their support in diverse ways towards my education and to my brother, Robert Tetteh Djimajor whose support in these two years of my studies has been absolutely phenomenal. Also, to Sarah Bartels, Josephine Afrifa, Susana Boateng, Sitsofe Atiafe, Dulcie Quist, Caroline Dodzi Iko and all my friends and loved ones for their support in diverse ways towards my studies.



## ACKNOWLEDGEMENT

My warmest gratitude goes to my supervisors Dr. G. K. Banini and Prof. S. B. Dampare whose efforts ensured that this research work saw the light of day. Your coaching and mentoring have been the very foundation of this research output and may posterity reward your good efforts.

My profound gratitude also goes to Mr. Christian Nuviadenu, Mr. Hyacinthe Ahiamadjie, Dr. Joseph Tandoh and Mr. Daniel Wordson all of NNRI, GAEC, for their immense support in diverse ways throughout the study period. I cannot say thank you enough to you Chris with regards to the elemental analysis of the samples overseas.

I also wish to thank Dr. F.G. Ofose and Rev. Dr. S.A. Bamford for their constructive criticisms and especially Dr. Ofose for time taken off your busy schedules to go through every bit of my work with me.

Finally, I wish to acknowledge my colleague students and all persons who contributed to the success of this research work. God bless you all!

## TABLE OF CONTENTS

DECLARATION	i
DEDICATION	ii
ACKNOWLEDGEMENTS	iii
TABLE OF CONTENTS	iv
LIST OF TABLES	vi
LIST OF FIGURES	vii
LIST OF ABBREVIATIONS	viii
ABSTRACT	ix
<b>CHAPTER ONE: INTRODUCTION</b>	
1.1 Background	1
1.2 Statement of the problem	4
1.3 Research Objectives	5
1.4 Relevance and Justification	5
1.5 Scope and Limitation	6
<b>CHAPTER TWO: LITERATURE REVIEW</b>	
2.1 An Overview	7
2.2 Source and Transport Mechanism	11
2.3 History of Aerosol Studies	12
2.4 Current Trends	14
2.5 Sampling Aerosol	14
2.6 Effects of Aerosols	17
2.7 Nuclear Analytical Techniques in Aerosol Studies	18
2.7.1 XRF Techniques in Aerosol Studies	19
2.8 Receptor Modeling in Aerosol Studies	23
2.8.1 Principal Component Analysis	23
2.9 Previous Aerosol Studies in Ghana	29

**CHAPTER THREE: MATERIALS AND METHODOLOGY**

3.1 An Overview	31
3.2 Materials	32
3.3 Sampling	34
3.4 Gravimetric Analysis	43
3.5 Laboratory Experiments	45
3.5.1 EDXRF Measurements	45
3.5.2 Calculations	46
3.6 Multivariate Receptor Modeling Analysis	48
3.7 Enrichment Factors	49

**CHAPTER FOUR: RESULTS AND DISCUSSIONS**

4.1 Gravimetric Analysis	51
4.2 Elemental Analysis	56
4.3 Multivariate Receptor Model	62
4.4 Enrichment Factors	70

**CHAPTER FIVE: CONCLUSION AND RECOMMENDATION**

5.1 Conclusion	72
5.2 Recommendations	73
<b>REFERENCES</b>	74
<b>APPENDICES</b>	81

## LIST OF TABLES

<b>Table</b>	<b>Page</b>
3.1 Details of field sampling information	41
3.7 Analytical parameters used for EDXRF measurements	46
4.1 Average aerosol mass concentration measured for Abuesi	51
4.2 International air quality standards and guidelines	53
4.3 VARIMAX rotated factor loading matrix of coarse mode aerosol	65
4.4 Elemental markers associated with the five major APM sources at Abuesi	69



## LIST OF FIGURES

<b>Figure</b>	<b>Page</b>
2.1 Atmospheric cycling of aerosols	10
2.2 Picture of some sources of airborne particulate matter	11
2.3 Schematic of a typical XRF spectrometry system	21
2.4 Typical spectra of WDXRF and EDXRF	22
3.1 Picture of a Gent sampler	32
3.2 Picture of a stacked filter unit	33
3.3 Picture of Epsilon 5 XRF machine	33
3.4 Picture showing an aerial view of the study location	36
3.5 Picture showing a fish smoking activity at Abuesi	36
3.6 Location map of the study area	37
4.1 Average mass concentrations for both coarse and fine aerosol samples	54
4.2 Variation of average CPM and FPM for days of the week	55
4.3 Variation of average CPM and FPM for three months	56
4.4 Typical fitted spectrum of coarse air filter sample using EDXRF	56
4.5 Average coarse mode aerosol elemental concentrations measured by EDXRF	57
4.6 Dendrogram showing the distribution of elements in the coarse aerosols	62
4.7 Plot of principal components of elements in the coarse mode aerosol	70
4.8 Enrichment Factor values calculated for the coarse mode aerosol	71



## LIST OF ABBREVIATIONS

APM	Airborne Particulate Matter
CPM	Coarse Mode Particulate Matter (PM <sub>2.5</sub> – PM <sub>10</sub> )
EDXRF	Energy Dispersive X-Ray Fluorescence
EF	Enrichment Factor
EPA	Environmental Protection Agency
FPM	Fine Mode Particulate Matter (PM <sub>2.5</sub> )
HCA	Hierarchical Cluster Analysis
IPM	Inhalable Particulate Matter (PM <sub>10</sub> )
PCA	Principal Component Analysis
PMF	Positive Matrix Factorization
SFU	Stacked Filter Unit
TSPM	Total Suspended Particulate Matter
WDXRF	Wavelength Dispersive X-Ray Fluorescence
WHO	World Health Organization
XRF	X-Ray Fluorescence Spectroscopy

## ABSTRACT

Airborne particulate matter (APM) composition has been studied at the Abuesi area. Aerosol samples in two size fractions were collected over a period of 3 months using the Gent stacked filter unit (SFU). Energy Dispersive X-ray Fluorescence Spectroscopy (EDXRF) was used to measure concentrations of up to 28 elements at the INFN-Accelerator Laboratory, University of Florence, Italy for the coarse fraction which accounted for 53.84 % of PM<sub>10</sub> aerosols in the Abuesi area. Mean values of 41.890  $\mu\text{g}/\text{m}^3$ , 22.469  $\mu\text{g}/\text{m}^3$  and 19.422  $\mu\text{g}/\text{m}^3$  were measured for Inhalable Particulate Matter (IPM/PM<sub>10</sub>), Coarse mode Particulate Matter (CPM) and Fine mode Particulate Matter (FPM) respectively and these were within the World Health Organisation (WHO) guidelines. Chlorine is established as an important component of the aerosol in Abuesi, originating mainly from sea spray. It accounted for 32.13 % of the total coarse mode aerosol elemental concentration. Characterisation of aerosols in the study area was performed using Principal Component Analysis (PCA) with VARIMAX rotation. Six factors score accounted for the three main identified APM sources (i.e. crustal material/soil dust, marine/sea spray and mechanical operations) in the area with crustal material/dust representing the dominant source. Enrichment Factor (EF) values also showed no enrichment for about 86 % of the measured elements with only Na which resulted predominantly from sea spray recording a moderate enrichment score of EF=3.386. The results obtained suggest that ambient air quality in the Abuesi area is safe. There is, however, the need to conduct further studies to estimate the black carbon concentrations of both fine and coarse aerosol fractions and, as well, investigate the elemental source profile of the various APM sources in the study area.

## CHAPTER ONE

### INTRODUCTION

#### 1.1 Background

Atmospheric aerosols are tiny particles suspended in the air. They occur naturally, originating from volcanoes, dust storms, forest and grassland fires, emissions from living vegetation, and sea spray. Human activities, such as the burning of fossil fuels and the alteration of natural surface cover, also generate aerosols. Averaged over the globe, anthropogenic aerosols (aerosols made by human activities) currently account for about 10% of the total amount, but most of this is concentrated in the northern hemisphere, especially downwind of industrial sites (Brasseur and Roeckner, 2005; Dentener et al., 2006; Hardin and Kahn, 2010).

Airborne Particulate Matter (APM) has been found to significantly contribute to atmospheric fine particle pollution and efforts to control or at least monitor it has been made the world all over. These particles are known to affect the earth's radiation balance by interacting with solar radiation and by participating in cloud formation (Seinfeld and Pandis, 1998; Haywood and Boucher, 2000; Capes et al., 2009). Furthermore, global climate change and more recently human health are significantly affected as well by these airborne particulates. In general, the predominant chemical components of APM are sulphate, nitrate, ammonium, sea salt, mineral dust, organic compounds, and black or elemental carbon (Poschl, 2002), each of which typically contributes about 10 – 30 % of the overall mass load. In atmospheric research the term “fine air particulate matter” is usually restricted to particles with aerodynamic diameters

$\leq 2.5 \mu\text{m}$  (PM<sub>2.5</sub>) whereas larger particles with aerodynamic diameters up to  $10 \mu\text{m}$  (PM<sub>10</sub>) are referred to as “coarse particulate matter”.

In recent years, fast urbanization of the world population has resulted in increased levels of air pollution from the concentration of industrial and road traffic activities in urban and suburban areas worldwide of which Abuesi, a suburban coastal community in the Shama District of the Western Region of Ghana is no exception. From the viewpoint of particle exposure, the role of traffic and industrial activities is emphasized because these particles are typically emitted in our immediate environment. In order to protect public health and the environment therefore, air quality standards (AQS) are often issued by institutions like the Environmental Protection Agency (EPA) with the aim of controlling and reducing APM levels in the environment. However, to achieve this; there is the need for continuous investigations to identify, characterize and apportion these aerosol sources contributing to the atmospheric fine particle pollution.

A better understanding of the role of atmospheric particles requires the ability to model and measure particles both in natural environments and in detailed laboratory studies. Nuclear analytical techniques to this end find many of their most important applications. X-ray fluorescence spectroscopy (XRF), particle induced x-ray emission (PIXE) and instrumental neutron activation analysis ( $k_0$ -INAA) are among the numerous nuclear and related analytical techniques commonly used to yield multi-elemental data in atmospheric aerosol studies (Almeida et al., 2006) and they have been proven to be very good techniques in quantifying the elemental content of aerosol samples.

Practically, using multivariate receptor modeling techniques, such as Positive Matrix Factorization (PMF), Principal Component Analysis (PCA), etc. can provide information about pollution sources especially as the quantity and quality of APM data increases. The fundamental principle of receptor modeling involves assuming a mass conservation and subsequently, using a mass balance analysis to identify and apportion sources of airborne particulate matter in the atmosphere (Hopke, 1985, 1991). In order to obtain data set for receptor modeling, individual chemical measurements can be performed at the receptor site which is usually done by collecting particulate matter on a filter and analyzing it for the elements and other constituents.

In the last few decades, studies in atmospheric aerosol research has been the focus of an intense, coordinated, global effort (IAEA, 1994), primarily to characterize the source contributions of these airborne particulates and also to ascertain their impact on the environment and human health in particular. In view of this, it has been found necessary to locally evaluate the atmospheric aerosol content in a Ghanaian community through the application of some nuclear analytical technique (EDXRF) using multivariate receptor modeling statistics. At the end of this present research, it is expected that the results obtained would serve as a basis for further studies for the development of a comprehensive understanding of the aerosol problem in a typical Ghanaian community.

## **1.2 Statement of the Problem**

The study location is a suburban coastal community located some several kilometers from the Accra–Takoradi highway in the Shama District of the Western Region of Ghana. Like many others in most developing countries, the study location lacks modern infrastructure and cannot boast of any industry. This notwithstanding, fumes generated by thermal generation power plants situated at Aboadze, about 1.5 kilometers from the study location could greatly impact the air quality in the area. Again, local livelihood activities such as smoking of fish and burning of firewood as well as vehicular traffic, among others, could most probably serve as potential sources of atmospheric aerosols in the area. The contributions from these sources to atmospheric fine particle pollution as well as their effects on human health and the environment cannot be overemphasized. Thus, a comprehensive study on the atmospheric aerosols contributed by these sources would be of immense value in understanding and providing institutions like the EPA with the required information in formulating more technical policies to address the pollution problem.



### **1.3 Research Objectives**

#### **1.3.1 Main Objective**

The overall aim of the research project is to investigate the atmospheric aerosol problem in Abuesi, a typical Ghanaian suburban coastal community.

#### **1.3.2 Specific Objectives**

The specific objectives of this work include the following:

1. To ascertain the level of Total Suspended Particulate Matter (TSPM) in the study location.
2. To assess the air quality in the study location
3. To ascertain the degree of fine particle contamination by APM using enrichment factors (EF).
4. To investigate the possible sources of airborne particulates in the study location.

#### **1.4 Relevance and Justification**

The effects of atmospheric aerosols in our immediate environment are of great public concern because of their impact on the ecosystem. A combination of their physical and chemical characteristics, residence time in the atmosphere and transport mechanisms from sources (natural and anthropogenic) make these airborne particulates a serious threat to human life and the environment. Although their effects are predominant in heavily industrialized cities or countries, less or none industrialized towns and villages cannot claim immunity to their presence and subsequent effects. In Ghana, the periodic

assessment of air quality by the EPA involves only gravimetric analysis to ascertain the mass of TSPM across the country. This undoubtedly limits the depth of our understanding of these atmospheric particles in terms of their elemental composition, individual source contributions and their subsequent impact on the environment and human health. A comprehensive understanding of airborne particulates typically requires that, gravimetric analyses are complemented with multi-elemental analysis and receptor modeling statistics.

There is the need to assess the atmospheric aerosols present in the study area to determine the TSPM in the vicinity, their concentration and/or level of contamination and the possible sources of these airborne particulates which to a large extent can provide a basis for further studies in the field to better understand the aerosol problem. Data obtained from the analytical procedures would be invaluable in assessing the air quality of the study location.

### **1.5 Scope and Limitation**

This study was carried out in the Abuesi coastal community of the Shama District in the Western Region of Ghana. Atmospheric aerosol samples were collected using a Gent sampler by means of Nuclepore polycarbonate filters to determine the TSPM in the study location. In particular, parameters such as mass and mass concentrations of the TSPM as well as elemental concentrations of the airborne particulates were determined. The aerosol samples collection was carried out over a period of three months beginning from October to December, 2012 (i.e. during the predominant dry/harmattan season in Ghana) on a continuous monitoring basis.



## CHAPTER TWO

### LITERATURE REVIEW

#### 2.1 An Overview

Atmospheric aerosol particles constitute an important component of ambient air constituents. Several researchers show that aerosols have an adverse effect on human health and can be effective pathways for deposition of pollutants and exchange of nutrients. Toxic and trace element composition in the fraction of 10  $\mu\text{m}$  or less in diameter of particulate matter can easily be inhaled by humans (particularly particles less than 2.5  $\mu\text{m}$ ), thereby affecting human health. These particles are easily transported over long distances from their origin, and have importance also in their effect on climate and visibility. Basically, airborne particulates are classified by their aerodynamic diameter size and chemical composition. In terms of aerodynamic size, they are classified into fine particulates [i.e. particles with aerodynamic diameters  $\leq 2.5$   $\mu\text{m}$  (PM<sub>2.5</sub>)] and coarse particulates [i.e. larger particles up to 10  $\mu\text{m}$  (PM<sub>10</sub>)]. In terms of chemical composition, particulate matter is classified into two categories, primary and secondary particles. Primary particles are composed of particles that are emitted directly into the atmosphere from sources such as sea spray, road traffic and industry whereas secondary particulates are those occurring from the production of chemical transformation of SO<sub>2</sub>, NO<sub>x</sub>, HCl and ammonium compounds under atmospheric conditions (Panyacosit, 2000). Currently, air pollution studies involve collecting samples of air particulate matter using filters, determining the amount of suspended particulate matter ( $\mu\text{g m}^{-3}$ ) and analyzing the air filter samples for elemental

concentrations using some analytical technique(s). A comprehensive study of aerosols requires basically three major steps.

- 1. Sampling and gravimetric analysis:** This involves collecting aerosol samples using filters (e.g., Nuclepore, Teflon, etc.), by means of some kind of air suction machine such as Gent Sampler or High Volume Sampler among others. The gravimetric analysis of the Nuclepore filters is calculated by finding the difference in weights of each filter before and after sampling with a microbalance of very good sensitivity. It is strongly recommended to weigh the filters before and after sampling using a microbalance to obtain a proper weight of the amount of loading (i.e., sample mass).
- 2. Elemental analysis:** It involves the application of some analytical technique(s). Depending upon the sample type, the samples are analyzed by one or more of the following bulk analytical techniques including (but not necessarily limited to): Particle-Induced X-ray Emission analysis (PIXE) for measuring elements with atomic number above  $Z=10$ , Instrumental Neutron Activation Analysis (INAA) for elements with  $Z>10$ , X-ray Fluorescence Spectrometry (XRF) for elements with  $Z>10$ , Ion Chromatography (IC) for measuring ammonium, nitrate, sulfate and some other anionic and cationic species, a light reflectance technique (for determining black carbon), etc. The technique to employ for a particular analysis depends on several factors including filter type used for sampling, element of interest being investigated by the researcher, among others. The application of any of the above analytical techniques, however, provides as a rule, multi-species data sets for the sample(s) being analyzed.

- 3. Receptor modeling studies:** For a more thorough evaluation of the multi-element data sets for the series of samples, we take advantage of the receptor modeling techniques which make use of a numerical tool to describe the causal relationship between emissions, meteorology, atmospheric concentrations, deposition, and other factors. Primarily, they consist of mathematical models that focus on the description of the behaviour of airborne particulate matter in the environment. A well computed receptor modeling algorithm can give a more complete deterministic description of the aerosol problem, including an analysis of factors and causes and in some instances, guidance on the implementation of mitigation measures.

Understanding the role and effects of atmospheric particles requires the ability to model and measure particles both in natural environments and in detailed laboratory studies. To achieve this, there is the need to first understand their life cycle, quantitatively predict their emission, transportation and transformation. The elemental and chemical composition of aerosols is extremely variable with location, as well as time; and its contribution to air pollution and subsequent effects on the environment and human health is so immense such that more and more countries the world over continue to invest abundant scientific funds in investigating the properties and behaviour of aerosols (Mureley, 1991). This mainly includes study of the chemical composition of aerosols, the formation and transformation mechanisms and its effects on climate and human health. However, if realistic models are to be developed for air monitoring research, there is a need for systematic studies of airborne particulate matter. In Ghana for instance, the EPA undertakes periodic monitoring of the air quality across the country by means of a high volume sampler and quartz filters (to ascertain the total

suspended particulate matter in the atmosphere without any such further study for the characterization and/or apportionment of the aerosol particles).

Figure 2.1 is a diagram of the life cycle of aerosols in the atmosphere, showing emission, deposition and transport processes and the action of aerosols while in the atmosphere. Airborne particles undergo various physical and chemical interactions and transformations (atmospheric aging), which subsequently results in changes in their size, structure and composition.

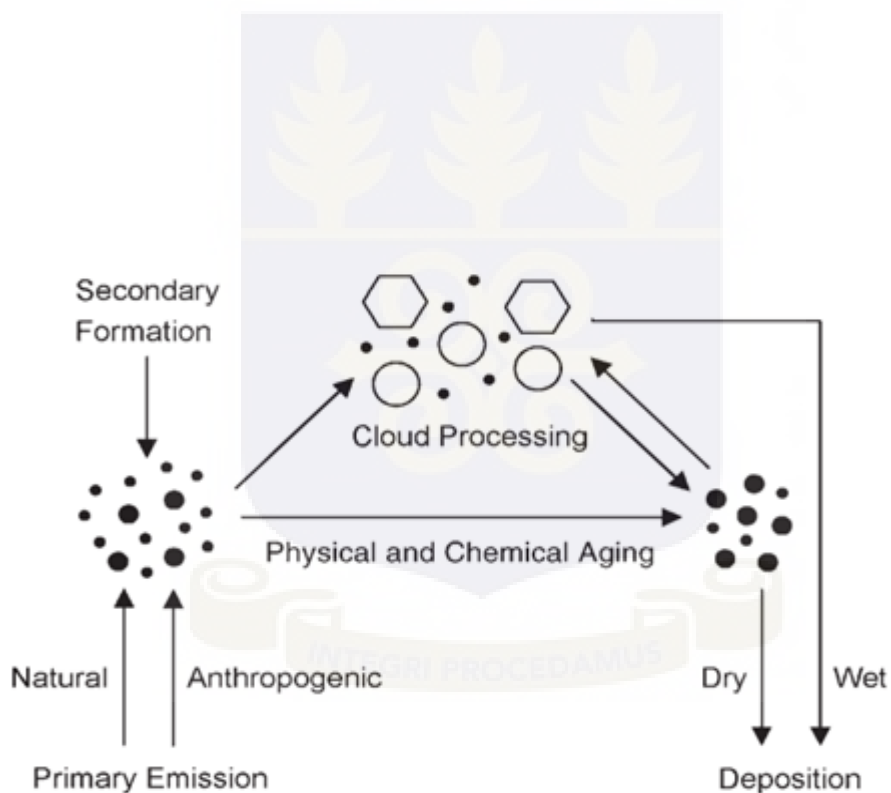


Figure 2.1: Atmospheric cycling of aerosols (after Panyacosit, 2000)

## 2.2 Source and Transport Mechanism



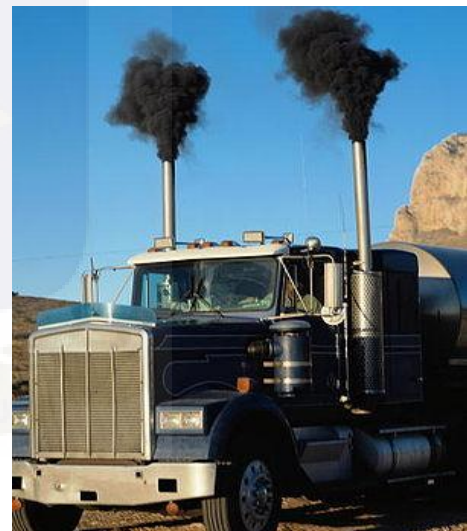
Fumes from industry



Windblown dust



Smoke from forest fires



Smoke from vehicular exhaust

*Figure 2.2: Pictures of some sources of airborne particulate matter*

APM in the troposphere and the atmosphere are subjected to worldwide distribution by air mass circulation and they are ultimately returned to the Earth's surface by wet deposition through precipitation and by dry deposition through sedimentation,

impaction and diffusion. The long-range transport of pollutants and subsequent influence in regions far from source areas has been extensively documented by many researchers. For instance, Europe, with its industrialized countries, is a strong source of anthropogenic emissions and already, effects of emissions from Europe have been detected in areas such as the Black Sea (Hacsalihoglu et al., 1992). According to Harris (1976), the variation of the size distribution of aerosol particles with the components and conditions is one of the best diagnostic tools to identify sources and history of the aerosol. Begum et al. (2010) noted that, understanding the possible contribution of regional or transboundary sources to local pollution sources, especially during wintertime, requires efforts to identify possible potential source regions and pathways of transboundary transport. Although a variation of the total mass loading with time and location exist, more important is the varied distribution of components throughout the particle size range, either as complete particles or smaller particles collected in or on particles, or a mixture.

### **2.3 History of Aerosol Studies**

Atmospheric aerosols have a rich history; with atmospheric aerosol science (i.e. the explanations of the origin, pattern and properties) emerging predominantly in the era of enlightenment (i.e., 1700-1800 AD). The origin of atmospheric aerosols was initially attributed to earthquakes, thunderstorm lightning, meteoric dust as well as to volcanoes, windblown dust and combustion processes. However, by the late 19<sup>th</sup> century, atmospheric observations and the use of simple physico-chemical principles allowed the consolidation of the then many ‘theories’; and this subsequently ruled out earthquakes, lightning and meteorites as significant sources of aerosols. Again, during this period,

the long-range transport of aerosols was well understood. Although, the scientific questions regarding atmospheric aerosols (such as their source, physical and chemical characteristics, effects, etc.) have not changed much over the past three centuries (Husar, 1990), the answers given to these questions have varied considerably. The 18<sup>th</sup> and 19<sup>th</sup> century saw mainly geologists studying atmospheric dust in connection with soil formation (Udden, 1896). Before the end of the 19<sup>th</sup> century, however, meteorologists had also come to appreciate the many influences that aerosols exert on the atmosphere. Although atmospheric aerosol science during the 20<sup>th</sup> century addressed all the topics of previous centuries, the methods of investigation, however, became increasingly quantitative and explicitly included the use of laws of physics and chemistry, such as conservation of mass and energy, as well as the laws of chemical kinetics. By the late 20<sup>th</sup> century, computational models have already been introduced to complement the many conceptual models. In summary, the 18<sup>th</sup> century was the beginning of modern scientific thinking on atmospheric aerosols whereas the 19<sup>th</sup> century saw the era of transition from theory-driven to observation-based atmospheric aerosol science. Theories were compared and qualitatively reconciled with systematic observations. The 20<sup>th</sup> century saw the development and application of several analytical techniques (elemental analysis) to comprehensively address the aerosol problem (i.e., in source characterization and apportionment). The 21<sup>st</sup> century experienced a major boost mainly as a result of governments and other agencies investing more funds into aerosol research, and by the use of some of the world's most sophisticated computational models to address the aerosol problem.

## **2.4 Current Trends in Aerosol Studies**

Atmospheric aerosol research is also a forefront and hotspot subject of current international atmospheric sciences (Crutzen, 1998). Scientific articles on aerosol research have demonstrated an expeditious increase in quantity over the past several decades (Jacobson, 2001; Andreae et al., 2006). During the last few decades, a great awareness has been created among the public and Governments as to the impact of chemical pollutants on the quality of human life and the general ecosystem. As a result, better understanding of the issues related to various aspects of environmental pollution in some parts of the globe previously thought to be “clean” are now found to contain hazardous pollutants like lead (Pb), mercury (Hg), etc. In the absence of general human activities in areas such as the Arctic, these pollutants might have been transported from distant sources (Amundsen et al., 1992). The developing world in this regard is in the early stage of undertaking such studies, and is limited to local factors, since most of these countries lack the funds, equipments and technical skills to execute such research programs. Today, with the use of sophisticated computer programming tools, understanding the aerosol problem is increasingly becoming more and more comprehensive.

## **2.5 Sampling Aerosol**

Sampling of APM has much to do with differentiating the size of the particles. Various sampling devices are used for the characterization of APM. Fundamentally, collection of TSPM can be achieved with or without size fractionation.



### **2.5.1 Collection of APM without size selection**

This type of sampler depends only on gravitational settling of particles. It involves the removal of particles on a collector in the absence of precipitation for dry deposition samples and removal of particles by precipitation for wet deposition. For TSPM collection, "high-volume" air samplers, with large volumes of air being drawn through a low resistance (glass or cellulose) filter are employed. Air flow ranges from 1.1 to 1.7 m/min, or about 2000 m/day. The inlet duct and collection filter measure 25 – 30 cm in diameter. This type of sampling is especially useful for monitoring of remote areas, which may have relatively low particulate concentrations, or for monitoring low-level products of anthropogenic nuclear activities.

### **2.5.2 Collection of APM with size selection**

These make use of samplers with physical/virtual impactor stages. Physical impactors operate on the principle of particle separation by size using "obstacles". Particles are removed onto solid surfaces using inertial forces and air flows around an obstacle (the impactor); and the particles in the airflow either follow the air stream or, depending on the mass (size) of the particle, impact on the obstacle, and are collected. Separations in samplers with virtual impactors occur at a "virtual" surface formed by diverging air streams. Coarse and fine particulates are then carried to separate filters. The size segregation of such devices is not as sharp as for physical impactors, and operation below about one micrometer appears difficult, but problems with collections surfaces are largely avoided.

### 2.5.3 Stacked filter units (SFU)

These types of samplers are operated at “medium” volume flow rate (about 18L/min) and use the principle of sequential filtration, where particle fractionation is achieved by partially efficient polycarbonate filters. These filters are utilized due to their specific particle capture behaviour for the desired size fractions and are located upstream of a pump in series.

The "Gent" SFU air sampler (employed in this study) is specifically designed for the collection of APM in the inhalable (PM<sub>10</sub>) size fraction, using the principle of sequential filtration. This sampler, designed at the University of Gent, Belgium (and currently being provided by Clarkson University, United States), is being used by many researchers including the International Atomic Energy Agency (IAEA) for co-ordinated research programmes in air pollution studies and related projects. The sampler uses an "open face" type stacked filter unit, in which two 47 mm Nuclepore polycarbonate filters (one filter of 8 µm pore size and the other of 0.4 µm pore size) are employed for the collection of APM. The filter unit is inserted in a cylindrical container, which is provided with a pre-impaction plate for the collection of particles larger than 10 µm. The sampler is designed to operate at a flow rate of approximately 18 L/min, where the pre-impaction stage provides a PM<sub>10</sub> cut-off point at standard temperature and pressure. At this flow rate, the coarse (8 µm pore size) Nuclepore filter collects the 2.5 – 10 µm size fraction, whereas the fine filter collects particles in the size range less than 2.5 µm.

A detailed description and instruction for the installation and use of the Gent SFU sampling equipment is given by Hopke et al. (1997) and Maenhaut (1992).

## 2.6 Effects of Aerosols

The effects of aerosols largely depend on their chemical composition (both the "bulk" composition and the composition as a function of particle size). Studies on atmospheric aerosols are of importance for various reasons due to problems caused by these elevated levels of APM. The importance such studies have been discussed below.

**Health:** Numerous epidemiological studies have documented that current day levels of APM are associated with adverse health effects, including increased risks of morbidity and mortality, mainly due to respiratory and cardio-vascular diseases (Pope and Dockery, 2006; Pope et al., 2002). According to WHO (2005) report, evidence of the association between airborne particulate matter and public health outcomes is consistent in showing adverse health effects at exposures experienced by urban populations in cities throughout the world, in both developed and developing countries. The risk for various outcomes has been shown to increase with exposure and there is little evidence for a threshold below which no adverse health effects would be anticipated.

**Climate:** Major gaseous components of atmospheric pollutants are important to study as they influence global climate change and acid precipitation while the particulate matter constituents, mostly the trace elements in different chemical forms, are also important to study as they influence cloud formation and solar radiation balance. APM according to Ramanathan and Carmichael (2008), can have either a cooling effect on the atmosphere through scattering of shortwave radiation (sulphate and organic carbon

particles) or a warming effect through absorption of shorter wave radiation (black carbon particles).

**Forest and Vegetation:** Vegetation exposed to wet and dry deposition of particulates may be injured when particulates are combined with other pollutants according to (World Bank Group, 1998) handbook on pollution prevention and abatement. Coarse particles, such as dust, directly deposited on leaf surfaces can reduce gas exchange and photosynthesis, leading to reduced plant growth. Also, heavy metals that may be present in particulates, when deposited on soil, inhibit the process in soil that makes nutrients available to plants.

In general, particulate emissions have their greatest impact on terrestrial ecosystems in the vicinity of emissions sources.

## **2.7 Nuclear and Related Analytical Techniques in Aerosol Studies**

The analysis of aerosols to determine primarily the elemental and some chemical constituents can be made by modern instrumental techniques. In particular a variety of methods are used to excite the atoms (Mueller and Kothny, 1973) whose radiation is characteristic of the elements, or by the effect of the particle on a beam of radiation or particles. Depending on the excitation mechanism, the characteristics of the radiation or beam after particle interaction, and the analyzing instrument; different names are often times used for the same technique or variations in the method. To this end, a wide range of methods can be and have been applied for the physical and chemical analysis of aerosol particles and components. In practice, the selection and

combination of analytical methods depend on the sample type and target parameters and requires a trade-off between sensitivity and selectivity. The Scanning Electron Microscope (SEM) is one of the oldest analytical techniques (McCrone and Delly, 1973), and although it basically only examines the surface, information on particle size, shape, texture and topography of the surface is obtained. The Electron Spectroscopy for Chemical Analysis (ESCA), on the other hand, uses ultraviolet or x-ray photons to excite outer shells of atoms leading to ejection of electrons whose kinetic energy is reduced by the chemical binding energy and can therefore be used to identify elements by their chemical binding energy. In many cases protons, high energetic alpha particles and/or gamma ray photons are used as the activating particles. There are many other related analytical techniques including x-ray fluorescence spectroscopy, particle induced x-ray emission, instrumental neutron activation analysis, ion probe, flame photometry, infrared spectra, etc. that can be applied to the aerosol problem. However, for the purposes of this study, the x-ray fluorescence spectroscopy will be further discussed with a review of literature on the analytical technique.

### **2.7.1 XRF Techniques in Aerosol Studies**

When an electron beam of high energy strikes a material, one of the results of the interaction between the electron beam and the material is the ejection of photoelectrons from the inner shells of the atoms making up the material. If the incident particle and binding energy are respectively  $(E)$  and  $(\phi)$  of the atomic electron in the material, the photoelectrons leave with a kinetic energy  $(E-\phi)$  which is the difference in the energies. This ejected electron leaves a “hole” in the electronic structure of the atom. The atomic electrons then rearrange, with an electron from a higher energy shell filling the vacancy.

By way of this relaxation the atom undergoes fluorescence, or the emission of an x-ray photon whose energy is equal to the difference in energies of the initial and final states. Detecting this photon and measuring its energy allows us to determine the element and specific electronic transition from which it originated (Jenkins, 1988).

XRF is a multielemental, non-destructive technique which can simultaneously determine up to over 30 elements in air filter samples. The technique involves the excitation of tightly bound electrons in the sample atoms by an x-ray generator and subsequently observing the x-ray emissions accompanying the de-excitation (Dzubay, 1977). In practice, XRF analysis of elements with  $Z > 10$  is highly efficient. By definition, the K-line of any element is the optimal spectral line to measure because of its superior sensitivity and reduced spectral interference. The basic concept of all spectrometer systems is a radiation source, a sample and a detection system. Spectrometer systems are generally divided into two main groups: energy dispersive systems (EDXRF) and wavelength dispersive systems (WDXRF). The difference between the two lies in the detection system. Several researchers have successfully employed XRF analysis in the study of atmospheric aerosols (e.g., Akoto Bamford et al., 2004; Hopke et al., 2008; Ofori et al., 2012).

### **Energy Dispersive X-ray Fluorescence Spectroscopy (EDXRF)**

XRF analysis, and especially the more nuclear related energy-dispersive version (EDXRF), allows for bulk analysis at the sub-ppm level, unifying for example, atmospheric aerosol studies and environmental particles in general (IAEA, 2009). In general, EDXRF analysis employs detectors that directly measure the energy as well as the intensity of the x-rays by collecting ionizations produced in a suitable detecting

medium. The x-ray tube acts as a source irradiating the sample directly, and the fluorescence emitted from the sample is measured with an energy dispersive detector. This detector is able to measure the different energies of the characteristic radiation emitted directly from the sample and can separate (disperse) the radiation from the sample into the radiation from the different elements present in the sample. This is as shown diagrammatically in Figure 2.3.

#### Advantages of EDXRF spectrometry

- i. Smaller, more compact instrument design
- ii. Less maintenance
- iii. Low electrical consumption
- iv. Improved system resolution
- v. Simultaneous elemental analysis

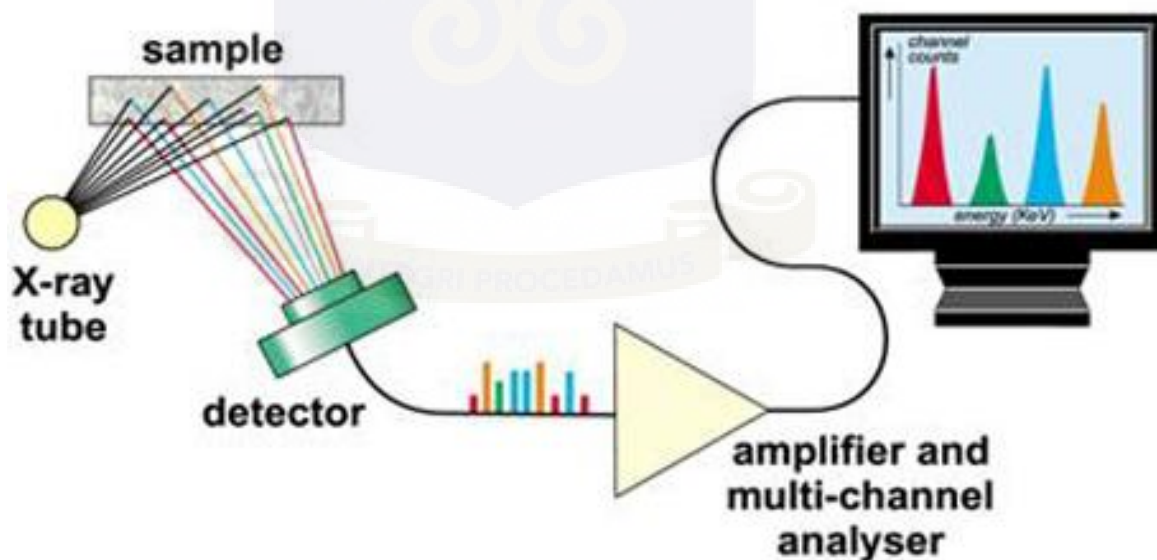


Figure 2.3: Schematic representation of a typical XRF Spectrometry system

### Comparison between EDXRF and WDXRF

The principal difference between EDXRF and WDXRF techniques lies in the achievable energy (spectral) resolution. The higher resolution of WDXRF provides advantages in reduced spectral overlaps, so that complex samples are more accurately characterized. However, the additional optical components of a WDXRF system (eg, diffracting crystal and collimators) means that it suffers from greatly reduced efficiency and as well, make for a relatively expensive instrument. Also with EDXRF an entire spectrum is acquired virtually simultaneously, thus allowing the detection of elements within a few seconds whereas in WDXRF, spectrum acquisition is made in a point by point fashion (which is extremely time consuming). Figure 2.4 shows a typical spectrum of both WDXRF and EDXRF systems.

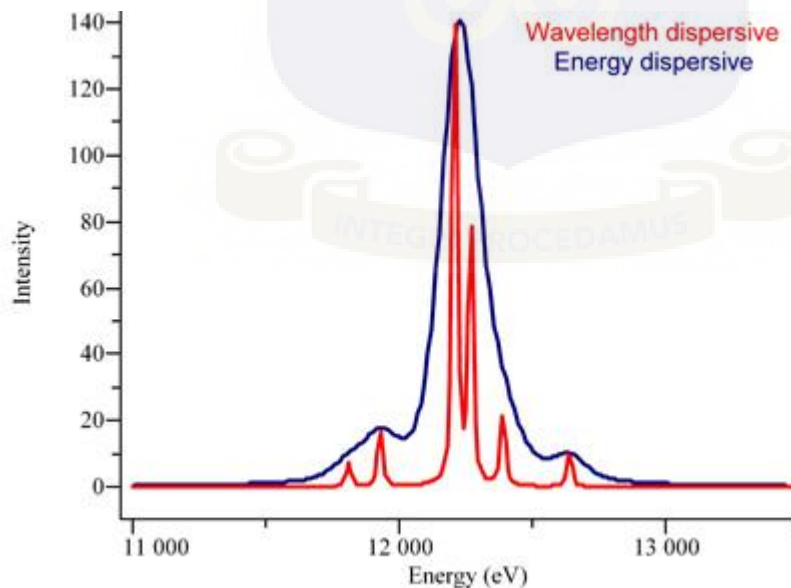


Figure 2.4 Typical spectra of WDXRF and EDXRF ([www.horiba.com](http://www.horiba.com), 11<sup>th</sup> April, 2013)



## **2.8 Receptor Modeling Techniques in Aerosol Studies**

Hopke (1985) reported that the elemental composition of particulate matter sources can be studied with the use of receptor models such as Chemical Mass Balance, Stepwise Multiple Regression, Factor Analysis, Cluster Analysis, etc. Alternative approaches have as well been developed for identifying and quantitatively apportioning sources of airborne particles using multivariate statistical analysis. These include Absolute Principal Factor Scores (APFS) which obtains the elemental mass contribution of each identified component by calculating the APFS for each sample. The elemental concentrations are subsequently regressed on the APFS to obtain the contribution of each element for each component; Positive Matrix Factorization (PMF) which, according to Paatero (1997), is a model which assumes that a measured dataset conforms to a mass-balance of a number of constant source profiles, contributing varying concentrations over the time of the dataset (time series) among others. The importance of multivariate receptor modelling in aerosol studies is readily observed from literature with a great number of researchers employing this tool for statistical analysis of their dataset.

### **2.8.1 Principal Component Analysis (PCA)**

Principal components and factor analysis are names given to several of the variety of forms of eigenvector analysis which involves simplification of the description of a system by determining the minimum number of new variables necessary to reproduce the measured attributes of that system. The first step in the eigenvector analysis is the calculation of a dispersion matrix, the matrix that contains quantitative information on the relative variation of pairs of variables or samples (cases). One of two kinds of

dispersion matrices, the covariance matrix unlike the correlation matrix, does not require scaling of the data set. For many types of data sets, the covariance matrix is applied because each variable has the same measurement scale. In principal factor analysis, a model of the variability of the trace element concentrations is constructed so that the set of intercorrelated variables is transformed into a set of independent, uncorrelated variables (Harman, 1976). This is done by finding the eigenvalues and eigenvectors of the correlation matrix. The most prominent eigenvectors (factors) are retained and orthogonally rotated by a VARIMAX rotation. The resulting "factor-loading" matrix represents the correlations between the trace elements and each orthogonal factor. Factor scores can further be calculated which indicate the relative importance of each factor for the individual samples.

In principle, the goals of PCA are to (a) extract the most important information from the data set, (b) compress the size of the data set by keeping only this important information, (c) simplify the description of the data set, and (d) analyze the structure of the observations and variables. In order to achieve these goals, PCA computes new variables called principal components which are obtained as linear combinations of the original variables. The first principal component is usually required to have the largest possible variance whereas the second component is computed under the constraint of being orthogonal to the first and so on. The values of these new variables for the observations are called factor scores, which can be interpreted geometrically as the projections of the observations onto the principal components.

### Mathematical formulations

The fundamentals of PCA theorem lies in the ability to extract the most important information from a large set of data using some mathematical projections and to express this information as a set of new orthogonal variables called principal components. Generally speaking, PCA uses a vector space transform to reduce the dimensionality of these large data sets. Assume that we start with a data set that is represented in terms of a  $M \times N$  matrix,  $X$  where the  $N$  columns are the samples (e.g., observations) and the  $M$  rows are the variables. We wish to linearly transform this matrix,  $X$  into another matrix,  $Y$ , also of dimension  $M \times N$ , so that for some  $M \times M$  matrix,  $P$  ;

$$Y = PX \quad (2.1)$$

This equation represents a change of basis. If we consider the rows of  $P$  to be the row vectors  $p_1, p_2, \dots, p_m$  and the columns of  $X$  given by  $x_1, x_2, \dots, x_n$  ; then equation (2.1) above can be interpreted in the following way:

$$Y = PX = (px_1, px_2 \dots px_n) = \begin{bmatrix} p_1x_1 & p_1x_2 \dots & p_1x_n \\ p_2x_1 & p_2x_2 \dots & p_2x_n \\ p_mx_1 & p_mx_2 \dots & p_mx_n \end{bmatrix} \quad (2.2)$$

This indicates that the original data,  $X$  is being projected on to the columns of  $P$ . Thus, the rows of  $P$ ,  $\{p_1, p_2, \dots, p_m\}$  are a new basis for representing the columns of  $X$  which subsequently are transformed into the principal component.

To obtain our components, let  $X$  now represent a matrix with singular value decomposition of a data set given by:

$$X = P\Delta Q^T \quad (2.3)$$

From equation (2.3), the factor scores matrix, denoted  $F$  is obtained as

$$F = P\Delta \quad (2.4)$$

The matrix  $Q$  gives the coefficients of the linear combinations used to compute the factors scores. This matrix can also be interpreted as a projection matrix because multiplying  $X$  by  $Q$  gives the values of the projections of the observations on the principal components. This is obtained by combining equations (2.3) and (2.4) to give equation (2.5), presented as:

$$F = P\Delta = P\Delta Q Q^T = XQ \quad (2.5)$$

The matrix  $Q$  is also called a loading matrix. The components can as well be represented geometrically by the rotation of the original axes. In this context, the matrix  $X$  can be interpreted as the product of the factors score matrix by the loading matrix as:

$$X = FQ^T \text{ with } F^T F = \Delta^2 \text{ and } Q^T Q = 1 \quad (2.6)$$

Also, the eigenvalue associated to a component is equal to the sum of the squared factor scores for that component and, therefore, the importance of an observation for a component can be obtained by the ratio of the squared factor score of this observation to the eigenvalue associated with that component. This ratio is called the contribution of the observation to the component. Formally, the contribution of observation  $i$  to component  $l'$  denoted  $C_{i,l'}$  can be defined as:

$$C_{i,l} = \frac{f_{i,l}^2}{\sum_i f_{i,l}^2} = \frac{f_{i,l}^2}{\lambda_l} \quad (2.7)$$

where  $\lambda_l$  is the eigenvalue of the  $l^{th}$  component.

The value of a contribution is between 0 and 1, and for a given component, the sum of the contributions of all observations is equal to unity. The larger the value of the contribution, the more the observation contributes to the component.

Since only the important information needs to be extracted from a data matrix, a problem arises when using PCA regarding the number of components that needs to be considered. Some useful guidelines regarding a solution to this problem have been proposed by several researchers (e.g., Jackson, 1991; Jolliffe, 2002). A first procedure according to Jolliffe (2002), is to plot the eigenvalues according to their size (the so called “scree plot”) and to see if there is a point in this graph (often called an “elbow”) such that the slope of the graph goes from steep to crosswise and to keep only the components which are before the elbow. This procedure is somewhat subjective. Another standard tradition is to keep only the components whose eigenvalue is larger than the average eigenvalue (which is the case employed in this study).

According to Abdi (2003), interpretation of the obtained components often involves some form of rotation of the components that were retained. Two main types of rotation are used:

**a) Orthogonal rotation**

An orthogonal rotation is specified by a rotation matrix in which the rows stand for the original factors and the columns for the new (rotated) factors. At the

intersection of row  $m$  and column  $n$  we have the cosine of the angle between the original axis and the new one given by:

$$r_{m:n} = \cos\theta_{m,n} \quad (2.8)$$

A rotation matrix has the important property of being orthonormal because it corresponds to a matrix of direction cosines. VARIMAX rotation, a popular method developed by Kaiser (1958), involves a simple solution in which each component has a small number of large loadings and a large number of zero (or small) loadings. This simplifies interpretation because, after a VARIMAX rotation, each original variable tends to be associated with one (or a small number) of components, and each component represents only a small number of variables. In addition, the components can often be interpreted from the opposition of few variables with positive loadings to few variables with negative loadings. Formally, VARIMAX searches for a linear combination of the original factors such that the variance of the squared loadings is maximized, which amounts to maximizing

$$V = \sum(q_{j,l}^2 - q_l^2) \quad (2.9)$$

where;

$q_{j,l}^2 =$  squared loading of the  $j^{\text{th}}$  variable of matrix  $Q$  on component,  $l$

$q_l^2 =$  mean of the squared loadings

### **b) Oblique rotation**

With oblique rotations, the new axes are free to take any position in the component space, but the degree of correlation allowed among factors is small because two highly correlated components are better interpreted as only one factor. Oblique rotations, therefore, relax the orthogonality constraint in order to gain simplicity in the interpretation. This method of rotation was strongly recommended by Thurstone (1947), but is rarely used compared to their orthogonal counterparts.

The relevance of the rotation in facilitating the interpretation is readily observed when the data follow a model (such as the psychometric model) in which each variable load on only one factor and/or that there is a clear difference in intensity between the relevant factors (whose eigenvalues are clearly larger than one), then the rotation is likely to provide a solution that is more reliable than the original solution. However if this model does not accurately represent the data, then rotation will rather make the solution less replicable and potentially harder to interpret due to loss of the mathematical properties of the PCA model.

## **2.9 Previous Aerosol Studies in Ghana**

As indicated earlier, atmospheric aerosol research is a forefront and hotspot subject of current international atmospheric sciences, and researchers in Ghana for over a decade, have been involved in cutting edge investigations in this field of scientific research.

In their investigation of biomass burning contribution to ambient air particulate levels, Ofose et al. (2013), measured the concentrations of APM in Navrongo, a town in the

Sahel Savannah Zone of Ghana and as well identified the major sources. Elemental and organic carbon concentrations were determined using Thermal Optical Reflectance methods whilst concentrations of elements were measured by energy-dispersive X-ray fluorescence. Average PM<sub>2.5</sub> mass concentration of 32.3 µg/m<sup>3</sup> was reported for the Navrongo area with total carbon contributing about 40 %. Biomass combustion was also identified as second most important source next to soil dust at Navrongo in their study.

Again, PMF was used to identify up to eight sources including industrial emissions, fresh sea salt, diesel emissions, biomass burning, two stroke engines, gasoline emissions, aged sea salt, and soil dust of airborne fine particles in the PM<sub>2.5</sub> range at Ashaiman, a suburban town north of Tema in Ghana (Ofosu et al., 2012). In this study, fossil fuel and biomass combustion as well as the presence of harbour and industries located at Tema were observed to have substantial impacts on inhalable APM concentrations in the Ashaiman area.

In 2008, Dotse et al., (2012) also investigated the particulate matter and black carbon concentration levels in Ashaiman. Average mass concentration values of 23.06 µg/m<sup>3</sup> and 96.56 µg/m<sup>3</sup> were reported for PM<sub>2.5</sub> and PM<sub>10</sub> respectively.

Boamponsem et al., (2010) also investigated the deposition of atmospheric heavy metals in the gold mining town of Tarkwa in Ghana. In this particular study, total heavy metal concentrations were measured by Instrumental Neutron Activation Analysis (INAA) and processed by PMF, PCA and Cluster Analysis (CA). Agricultural activities, natural soil dust and gold mining activities were identified as the main contributors of heavy metals in the atmosphere of the study area.



## CHAPTER THREE

### MATERIALS AND METHODOLOGY

#### 3.1 An Overview

The research methodology primarily consisted of field work (sampling), laboratory experimentations and theoretical analytical methods. The aerosol samples were collected in a neighbourhood located along the west coast of Ghana, characterized by relatively low vehicular traffic and commercial activities as well as hilly areas and coastal shrub vegetation. All the measurements were taken during the harmattan period in 2012. Specifically, the sampling station was studied for APM over a period of approximately three months (i.e. October to December). The specific sampling station was carefully selected to best represent the suspended PM collected in the study location in order to reveal the actual concentration levels of TSPM in the area. The 24 hour outdoor measurements of PM<sub>10</sub> and PM<sub>2.5</sub> mass concentrations were conducted with the use of a Gent SFU, at a flow rate of approximately 17 Litres per minute. The sampler was positioned on top of a bluff at about 3 metres high above the ground. The results and observations recorded during the entire process are as presented and discussed in the sections that follow. In summary, the procedure and/or methodology employed to obtain the expected results of the research problem included:

- i. Sampling (i.e. aerosol sample collection using a Gent SFU on a continuous monitoring basis)
- ii. Gravimetric Analysis (i.e. determination of air particulate mass concentrations)
- iii. Multielemental analysis by XRF technique

- iv. Data analysis (i.e. involving the application of receptor modeling techniques such PCA and Enrichment Factors)

### 3.2 Materials

The equipment employed in this study are shown in Figures 3.1, 3.2 and 3.3.

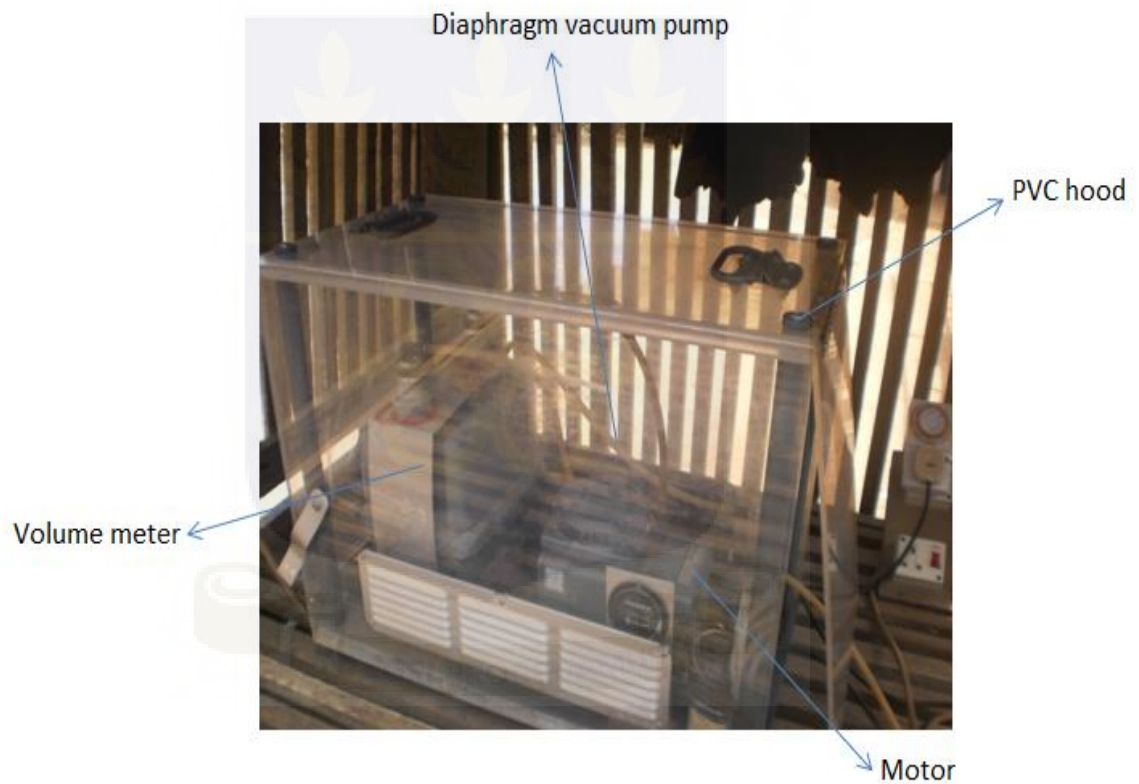


*Figure 3.1: Gent Sampler*



*Figure 3.2: Stacked Filter Unit (SFU)*



*Figure 3.3: Epsilon 5 XRF machine showing sample chamber*

### **3.3 Sampling**

#### **3.3.1 Sampling Equipment**

Devices for aerosol sampling commonly make use of filters and impaction stages; and the approach in this particular study was no different. A Gent stacked filter unit (SFU) sampler was used for collecting the atmospheric aerosol samples at a flow rate of approximately 17 liters per min (L/min). The SFU uses an inlet that provided a 50% cut-off diameter of 10  $\mu\text{m}$ . The particulates with an Equivalent Aerodynamic Diameter (EAD) of less than 10  $\mu\text{m}$  were collected in separate "coarse" (2.5 – 10  $\mu\text{m}$ ) and "fine" (<2.5  $\mu\text{m}$ ) size fractions on two sequential 47 mm diameter Nuclepore polycarbonate filters. The discrimination against the >10  $\mu\text{m}$  particles was accomplished by a PM10 pre-impaction stage upstream of the stacked filter cassette. Notably, the air was drawn through the sampler by means of a diaphragm vacuum pump, enclosed in a special housing together with a needle valve, vacuum gauge, flow meter, volume meter, time switch (for interrupted sampling) and hour meter.

#### **3.3.2 Receptor Site**

A Gent stacked filter unit (SFU) was used to collect aerosol particles from the suburban coastal area of Abuesi in the Shama District of the Western Region of Ghana. The study area is situated along the west coast of the Atlantic Ocean and located a few kilometres from vehicular traffic along the Accra–Takoradi highway and several kilometres from the heavy-traffic of the oil-rich Takoradi Metropolis area. The main industrial activity with a potential of affecting the air quality of the study area is the 350 MW Takoradi Thermal Power Station (which is situated at Aboadze, just about 1 km from the study location) whereas the main point source in the area, fish smoking by fishmongers along

the coastal belt of the vicinity is located about 100 m south to the sampling station. Other major local sources include firewood burning, vehicular traffic, and sources from the sea spray among others. Although the study location may not be immediately affected by the industrial pollution from the Thermal Plants, there is still the potential to be affected by the long range fine particle pollution transport occurring from generator fumes from the thermal plants as well as combustion from vehicular traffic along the Accra–Takoradi highway.

The sampling station was located upwind from local sources originating from the community's central business area along the sea coast. The station was carefully selected to best represent the local environments (e.g., topography, micrometeorology) and local particle sources (e.g., vehicular traffic, residential firewood burning for domestic purposes, fish smoking, etc.) in the vicinity of the study location.

The study location experiences a moderate climate with relatively mild temperatures ranging between 22 °C and 28 °C, and there are small hills in the rear of the sampling site. Although the community experiences a relatively calm period throughout the day, strong southerly winds along the coast aided by local topographical factors characterise the 24 hour daily cycle of the vicinity. This eventually gives rise to local flows and subsequent transport of APM thereby affecting the air quality in the area. Figures 3.4, 3.5 and 3.6 show fish smoking activities and aerial view of the community as well as location map of the study area.



*Figure 3.4: An aerial view of the study location (Abuesi)*

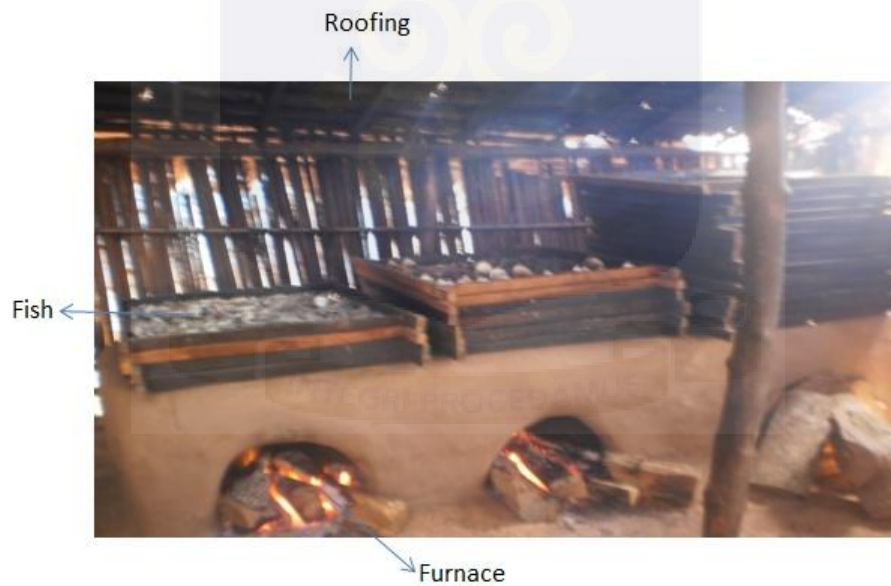


*Figure 3.5: Fish smoking activity at Abuesi*

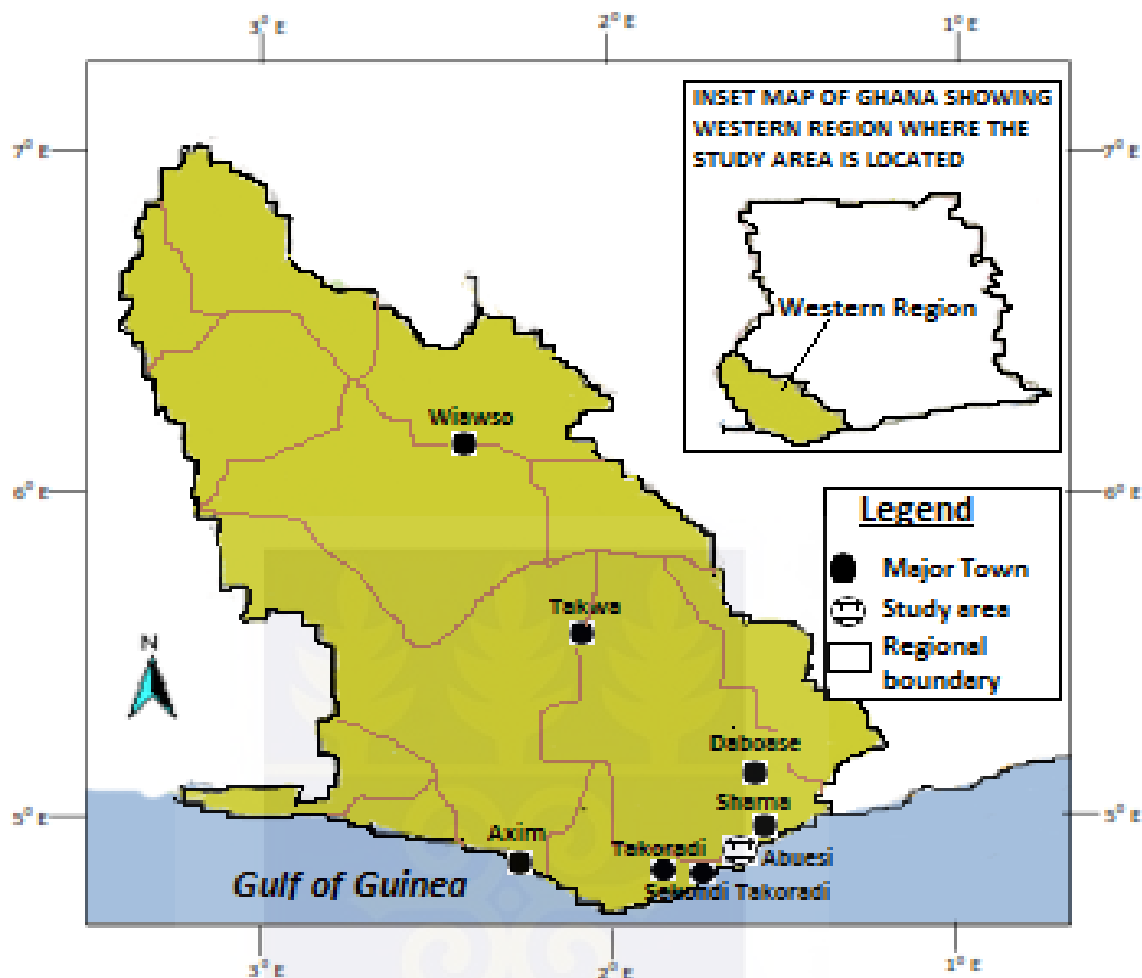


Figure 3.6: Location map of the study area

### 3.3.3 Sampling Protocol

After obtaining the desired filters, they were kept in a desiccator under a conditioning environment ( $20\text{ }^{\circ}\text{C} \pm 2\text{ }^{\circ}\text{C}$  and relative humidity of about  $50\% \pm 5\%$ ) for 24 hours before weighing to determine the actual weights of the empty filters. Each filter was then permanently identified by a serial number coding using a permanent marker on the petri dishes housing each of the filters. Care was taken to ensure consistency in the identification codes encrypted on each petri dish to avoid repetition and misidentification of the filters. The filters were then inspected visually for holes, tears,

particles and other imperfections that may cause uneven loading, loss of particulate matter, or other failure during the sampling process.

Installation of the “clean” empty filters in the Gent SFU was carefully executed. Firstly, the wing nuts of the stack filter cassette were loosened and the faceplate removed. By means of forceps, the filters were gently picked and with its shiny surface up, placed in center position in the filter holder in the cassette so that the gasket forms an airtight seal on the outer edge of the filter when the faceplate is in position. The faceplate was then replaced and the wing nuts tightened. Care was taken to ensure that the gasket was not tightened to the point that filter damage might occur. Installation and removal of filters during the entire sampling period was performed inside a clean enclosed building, thus eliminating handling problems due to lack of space and windy conditions.

The first filter holder of the cassette (i.e., the holder that faces the air intake) was loaded with a "coarse" filter; whereas the second filter holder of the cassette was loaded with a "fine" filter. This was done to ensure that aerosol particles with aerodynamic diameters  $<2.5 \mu\text{m}$  were collected after successfully passing through the coarse filter un-trapped. Both the "coarse" and "fine" filters had their shiny surfaces up (thus, facing the air intake). Approximately, filter area of about  $12.571 \text{ cm}^2$  was exposed to the air flow during sampling (for both the coarse and fine filters). The stacked filter cassette was also properly tightened after loading to avoid any tripping occurrences during the sampling process.

All the aerosol samples were collected on Nuclepore polycarbonate filters with  $0.8 \mu\text{m}$  pores for the coarse fractions and  $0.4 \mu\text{m}$  pores for the fine fractions using a Gent stack sampler (Nuclepore, supplied by Whatman International Ltd, Maidstone, England). The



SFU sampler with a rain protective covering was mounted on a wooden post near the Abuesi SDA Basic School compound at approximately 3 meters high above the ground on top of a bluff at about 50 meters above sea level. Specifically, the sampler was mounted such that, the air flow around it was unobstructed. The sampler was programmed to run automatically at an air flow rate of approximately 17 litres per minute to collect the two size aerosol fractions ( $<2.5 \mu\text{m}$  and  $2.5 - 10 \mu\text{m}$  aerodynamic diameter particles) over the 24 hour continuous monitoring period. A total of 25 samples for the two particle size fractions (i.e., each sample comprises one fine and one coarse) were collected at the sampling station. The total volume of air sampled through the filter was calculated from the reading of the average value of the initial and final flow rate.

After sampling, the filters were removed by means of biceps and gently placed in position in the already labeled petri dishes. This was done to minimize sample loss during transport to the laboratory for reweighing and analysis. The collected filter samples were immediately placed in polyethylene plastic bags right after sampling, transported back to Accra and reserved in a desiccator for approximately 24 hours before laboratory investigations were conducted. Prior to this, a visual inspection was conducted on each filter to check for holes or other physical damages and foreign materials (such as insect) which might have occurred during the sampling exercise since these have the potential of affecting the results of the samples during analysis. In either case, extreme caution was observed to avoid filter damage and/or contamination during placement and removal of the filters as well as removal of the faceplate and filter holder cassette.

The study location is moderately polluted as a result of community activities such as fish smoking, vehicular movement, burning of firewood and charcoal, windborne dust particles and air particulate mass contributions from sea spray, among others. Thus, although the sampling time was twenty-four (24) hours continuous, the sampler was operated on a 1 – 2 hours on and 1 hour off basis over the 24 hour monitoring period to avoid possible reduction in flow rate and filter clogging problems. This ensured that the sampler's aerodynamic characteristics were maintained throughout the sampling period for proper size fractionation and collection efficiency. In total 50 filter samples (i.e., 25 – “fine” and 25 – “coarse” filters) were collected on-site at the study location over the sampling period of about three (3) months. Details of the field sampling information are as summarized and presented in Table 3.1.

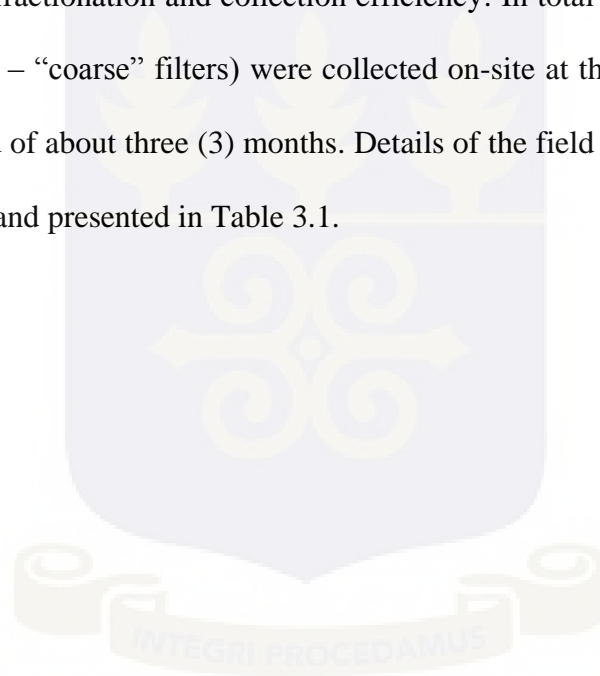


**Table 3.1: Detail of field sampling information with changes in atmospheric conditions and/or observations**

Filter ID	Time		Date		Flow Rate		Condition/Observation
	Start	Stop	From	To	Initial	Final	
1	5:00am	5:00am	10/18/2012	10/19/2012	17	17	Sunny Day
2	5:00am	5:00am	10/20/2012	10/21/2012	17	15	Rainy Day - Light Out
3	5:00am	5:00am	10/21/2012	10/22/2012	17	15	Sunny Day - Light Out (2X)
4	5:00am	5:00am	10/24/2012	10/25/2012	17	17	Rainy Day
5	5:00am	5:00am	10/25/2012	10/26/2012	17	17	Sunny Day
6	5:00am	5:00am	10/26/2012	10/27/2012	17	15	Sunny Day
7	5:00am	5:00am	10/31/2012	11/1/2012	17	17	Rainy Day - Light Out
8	5:00am	4:40am	11/20/2012	11/21/2012	17	15	Sunny Day - Light Out (4X)
9	5:00am	4:45am	11/21/2012	11/22/2012	17	15	Sunny Day - Light Out
10	5:00am	4:45am	11/22/2012	11/23/2012	17	17	Sunny Day - Light Out
11	5:00am	4:50am	11/23/2012	11/24/2012	17	17	Sunny Day - Light Out
12	5:00am	4:50am	11/24/2012	11/25/2012	17	17	Sunny Day
13	5:00am	4:50am	11/25/2012	11/26/2012	17	17	Sunny Day
14	5:00am	4:50am	11/26/2012	11/27/2012	17	17	Sunny Day - Light Out
15	5:00am	4:50am	11/27/2012	11/28/2012	17	17	Sunny Day - Light Out
16	5:00am	4:50am	11/28/2012	11/29/2012	17	17	Sunny Day - Light Out
17	5:00am	4:55am	12/2/2012	12/3/2012	17	17	Sunny Day
18	5:00am	4:55am	12/3/2012	12/4/2012	17	17	Sunny Day
19	5:00am	4:55am	12/4/2012	12/5/2012	17	17	Sunny Day - Light Out
20	5:00am	4:55am	12/5/2012	12/6/2012	17	17	Sunny Day - Light Out
21	5:00am	4:55am	12/6/2012	12/7/2012	17	17	Rainy Day
22	5:00am	4:55am	12/7/2012	12/8/2012	17	17	Sunny Day
23	5:00am	4:55am	12/8/2012	12/9/2012	17	17	Sunny Day - Light Out
24	5:00am	4:55am	12/9/2012	12/10/2012	17	17	Sunny Day
25	5:00am	4:55am	12/10/2012	12/11/2012	17	17	Sunny Day

*\*Filter ID corresponds to a pair of Coarse and Fine filters loaded in position of the filter holder of the cassette*

### **Sampling Period**

The APM samples providing the data for this study were obtained over a period of approximately three (3) months; specifically from October to December, 2012. Twenty-four hour representative samples were collected at the site (including but not limited to weekdays) using the Gent air sampler. In total, 25 sample pairs (each sample pair comprises one fine and one coarse fraction sample; resulting in a total of 50 samples) were collected at the sampling station.

### **Meteorological Condition**

In Ghana, the climate is generally characterized by high temperatures and relatively high humidity most of the year, and distinctly marked by seasonal variations in precipitation. According to meteorological conditions, the year can be divided into two seasons, wet (rainy) season (between May to August) and dry (harmattan) season (between October to March). The dry season, unlike the wet, is characterized by dry soil and air conditions, low relative humidity and in some rare cases, scanty or no rainfall. During these periods, prevailing north-east trade winds from the Sahara desert of northern Africa become moderately strong thereby aiding in the long range transport of atmospheric aerosols across sub-Saharan Africa. The suspension of particulate matter (especially dust particles) in the atmosphere during these periods increase and the case was no different within the vicinity of the study location. The samples were collected from the month of October to December which is predominantly characterised by these dry/harmattan weather conditions. Atmospheric conditions such as temperature, humidity, wind direction and wind velocity were not recorded during the sampling period. However, changes in

weather conditions were recorded regularly during the period as indicated in Table 3.1.

### **3.4 Gravimetric Analysis**

After sampling, the airtight petri dishes housing the filters were transported to the Ghana Standards Authority (Metrology Laboratory) in polyethylene plastic bags for re-weighing. Before the filters were weighed, they were equilibrated for approximately 24 hours in a conditioning environment ( $20 \pm 2$  °C, relative humidity of about  $50 \pm 5$  %) free of acidic or basic gases that might react with the filter material. This was done to ensure that conditions before the weighing of the loaded filters actually satisfy those conditions present during the initial weighing of the empty filters. In all, the post weighing of the sample filters was carried out over a period of about 48 hours.

The filters were taken directly from the conditioning chamber (desiccator) to the balance to minimize the risk of contamination. Again, forceps was used to gently pick each filter and carefully placed in position at the center of the balance sample holder. During weighing, each of the filters was allowed to settle in the non-turbulent flow sample holder for about 30 seconds before weighing to the nearest milligram. Measurements were repeated three times for each separate coarse and fine filter. The measured weights were then recorded against their corresponding filter IDs in separate coarse and fine tables (see appendices). Both the coarse and fine aerosol sample filter weights were determined by an analytical electronic microbalance (METTLER TOLEDO Model AX26 Comparator). The microbalance has an application range of (1 µg – 22 g), making it an ideal measuring instrument for this study.

The difference in the weighted averages for each filter (i.e., empty and loaded filters) was calculated using equation (3.1) below to determine the particulate mass deposited on each coarse and fine filter sample.

$$mPM = F_L - F_E \quad (3.1)$$

During sampling, a pre-calibrated linear mass flow meter was used to measure the flow rate as shown in Table 3.1. Therefore, the volume of air sampled was calculated using equation (3.2) as;

$$Vol = FR \times ST \quad (3.2)$$

Finally, equation (3.3) gave the corresponding mass concentrations of the suspended particulate matter collected.

$$cPM = \frac{mPM}{Vol} \quad (3.3)$$

where;

$cPM$  = particulate matter mass concentration ( $\mu g/m^3$ );

$mPM$  = net average mass of particulate matter collected onto filter ( $\mu g$ );

$Vol$  = the volume of air sampled ( $m^3$ );

$FR$  = flow rate (litre per min.);

$ST$  = sampling time (hrs);

$F_L$  = average weight of loaded filter ( $\mu g$ );

$F_E$  = average weight of empty filter ( $\mu g$ ).

Summary of the gravimetric results are as presented in Tables 3.2 – 3.6 in the appendices. All the procedures employed were strictly quality-controlled to avoid any possible contamination of the samples.

### **3.5 Laboratory Experiments**

After the gravimetric mass determination of the APM, about 20 of the coarse Nuclepore filters were further analyzed using XRF to determine their elemental concentrations. Specifically, the filters were analyzed using the PANalytical Epsilon 5 XRF machine (Figure 3.2) at the INFN-Accelerator Laboratory, University of Florence, Italy. 25 out of a total of 28 elements were measured with over 95 % detection in the entire samples analyzed.

#### **3.5.1 EDXRF Measurements**

Elemental concentrations were determined by energy dispersive X-ray fluorescence (ED-XRF) technique using the Epsilon 5 XRF machine (a non-destructive fully integrated high-resolution energy dispersive X-ray fluorescence spectrometer system, which combines advanced elemental excitation capabilities with sophisticated instrument control and analytical software design to deliver enhanced sensitivity and accuracy with significantly reduced backgrounds) which allowed the simultaneous detection of 28 elements in the entire 20 coarse filter samples. The ED-XRF has a “powerful” X-ray tube, a 3D polarizing geometry, up to 15 secondary targets and a high-resolution Ge-detector with detection limit of the order of a few  $\text{ng}/\text{cm}^2$  on the filter deposit. Micromatter standard reference samples (thin polymer films with pure element deposition) whose concentrations have been determined by the manufacturer and validated by NIST standards (SRM 2783 - Nuclepore filter with deposited PM10) were used for the quantitative calibration of the system. The calibration was established using a single standard and a blank for each element. The Epsilon 5 XRF machine allows for the direct measurement of

elemental concentrations of samples without any prior sample preparation. Thus, the filters were loaded in position in the sample holder (capsules) and analyzed for their elemental concentrations by adjusting the spectrometry system to the required settings. The homogeneous collection of particles unto the filter papers ensured a “smooth” ED-XRF analysis of the samples. The measurement parameters (conditions) used for the experiment are shown in Table 3.7. The average live time measurement per condition for all the elements was about 460 seconds.

**Table 3.7: Analytical parameters used for the measurements**

Elemental Range	Current (mA)	Measurement time (Seconds)
Na – Ca	20.0	600
Ti – Cr	17.1	300
Mn – Zn	12.0	300
Br - Mo; Pt – Pb	7.5	500
Pd – Ba	6.6	600

### 3.5.2 Calculations

The results obtained by the ED-XRF analysis represent the yield in count per second per milliampere (cps/mA) of each element measured. The measured yield of all 28 elements is as tabulated in Table 3.8 (see appendices) with their respective blank and standard concentrations per each measurement.

The concentrations ( $\mu\text{g}/\text{cm}^2$ ) of each element in the samples were calculated using equation (3.4) below:

$$[p \cdot t]_z = [p \cdot t]_{z, std} \frac{Y_z - Y_{z, blank}}{Y_{z, std} - Y_{z, std, blank}} (\mu\text{g}/\text{cm}^2) \quad (3.4)$$

To obtain the concentrations in microgram per cubic metre ( $\mu\text{g}/\text{m}^3$ ), the active area of the Nuclepore filter paper used for the aerosol sampling was first calculated using the relation;



$$A = \pi r^2 = \pi \frac{d^2}{4} \text{ (cm}^2\text{)}, \quad d = 4 \text{ cm} \quad (3.5)$$

This yielded a value of 12.571 cm<sup>2</sup>. Multiplying equation (3.4) by (3.5) thus yielded concentration in microgram (µg). That is:

$$[p.t]_z(\mu g) = [p.t]_z(\mu g/cm^2) \times A(cm^2) \quad (3.6)$$

where:

$[p.t]_z$  = concentration of element of interest (µg/m<sup>3</sup>);

$[p.t]_{z,std}$  = standard concentration of element of interest (µg/cm<sup>2</sup>);

$Y_z$  = yield of element of interest (cps/mA);

$Y_{z,blank}$  = yield of blank nuclepore filter (cps/mA);

$Y_{z,std}$  = yield of standard for element of interest (cps/mA);

$Y_{z,std,blank}$  = yield of standard blank mylar (cps/mA);

$A$  = active area of nuclepore filter for APM deposition (cm<sup>2</sup>);

$d$  = diameter of nuclepore filter (mm).

Finally the results of equation (3.6) were divided by the volume (m<sup>3</sup>) of air sampled by each filter to obtain the concentrations of the elements in microgram per cubic metre (µg/m<sup>3</sup>). Determination of the Lower Limit of Detection (LLD) for the measured elements was accomplished by use of equation (3.7) below.

$$Y_{LLD} = LLD = 3 \sqrt{\frac{A_T - A_N}{N_C}} \text{ (cps/mA)} \quad (3.7)$$

Equation (3.8) was then finally employed to obtain the concentrations of elements below the LLD.

$$[p.t]_{LLD} = [p.t]_{LLD,std} \frac{Y_{LLD}}{Y_{LLD,std}} (\mu g/cm^2) \quad (3.8)$$

where;

$Y_{LLD}$  = yield for the lower limit of detection (cps/mA)

$A_T$  = total (gross) peak area

$A_N$  = net peak area

$N_C$  = number of channels

$[p.t]_{LLD}$  = concentration of LLD ( $\mu g/cm^2$ )

Results of the EDXRF measurements (i.e., net yield per element) are presented in Table 3.8 in the Appendix.

### 3.6 Multivariate Receptor Modeling Analysis

The Principal Component Analysis (PCA) and Hierarchical Cluster Analysis (HCA) statistical methods were applied to the database obtained from the XRF analysis using SPSS software package for Windows (Version 16.0) for the multivariate analysis. The PCA with VARIMAX rotation on the elemental concentrations was used specifically to extract correlations between the variables and identify the possible sources contributing to the APM collected during the sampling period. The method of HCA also served the purpose of classifying the various groups of elements measured. Large differences in scaling were observed in the variables; hence, normalization was performed before computing proximities (and this was automatically executed by the HCA procedure). The normalization was achieved by transforming values of the elemental concentrations to log base 10 values before performing multivariate statistical analysis on the data. Additionally, the Ward's

method of clustering was applied by the use of the squared Euclidean distance as a measure. Likewise, each variable was normalized to unit variance and thus contributed equally. In this present work, only factors having an Eigenvalue >1 were retained for further analysis.

### 3.7 Enrichment Factors

In order to determine the characteristics (degree of contamination of APM by the measured elements) of the average elemental concentrations, Enrichment Factor (EF) values were calculated. This was done by standardizing the concentrations of the measured elements against a reference element, (one characterized by low occurrence variability, such as: Al, Fe, Ti, Si, Sr, K, etc.). The contents of these reference elements in samples have been established to predominantly originate almost exclusively from the earth's crust (Loska et al., 2005).

In this study, like many other works, (Deely and Fergusson, 1994; Schiff and Weisberg, 1999; Baptista Neto et al., 2000; Mucha et al., 2003), iron (Fe) was used as the reference element to differentiate natural from anthropogenic components because its content is unrelated to that of other metals. Composition of the reference element, Fe, employed in this work was obtained from a set of data by (Taylor, 1964).

By definition, enrichment factor is expressed as:

$$EF_{(i)} = \frac{[C_i/C_r]_{aerosol\ sample}}{[C_i/C_r]_{background}} \quad (3.10)$$

where;

$EF_{(i)}$  = enrichment factor of element of interest

$C_i$  = concentration of element of interest in sample and/or earth crust

$C_r$  = concentration of reference element in sample and/or earth crust

The degree of anthropogenic influence is interpreted as follows:

$EF < 2$  = depletion to minimal enrichment;

$EF 2-5$  = moderate enrichment;

$EF 5-20$  = significant enrichment;

$EF 20-40$  = very high enrichment;

$EF > 40$  = extremely high enrichment.

Increase in EF values indicates an increase in the contributions of anthropogenic sources (Sutherland, 2000). All EF values less than 1 (i.e.,  $EF < 1$ ) indicate no enrichment. Results of the calculated EF values are as shown in Table 3.10 in the Appendix alongside the range of measured elemental abundances.

## CHAPTER FOUR

## RESULTS AND DISCUSSIONS

## 4.1 Gravimetric Analysis

The average TSPM mass concentration measured in the study location as well as the ratios between the mass concentrations are shown in Table 4.1. The average PM10 value measured at Abuesi is relatively low ( $41.890 \mu\text{g}/\text{m}^3$ ) compared with standards indicating a large geographical spread of the atmospheric particle pollution in the area. The observed standard deviations also express the fluctuations in experimental conditions for the analytical methods. In particular, the standard deviation for the FPM could be the result of variations that occur due to changing weather conditions and human activities from one day to another.

The CPM and FPM averaged  $22.469 \mu\text{g}/\text{m}^3$  and  $19.422 \mu\text{g}/\text{m}^3$ , respectively, whereas the PM10 was  $41.890 \mu\text{g}/\text{m}^3$ . The aerosol mass concentration ratio for CPM-IPM was found to be about ten percent (10 %) higher than the FPM-IPM ratio which suggests that most of the aerosols measured during the sampling period were in the

**Table 4.1: Average aerosol mass concentration ( $\mu\text{g}/\text{m}^3$ ) measured for Abuesi**

TSPM Fraction	Minimum	Maximum	Mean	Standard Deviation
IPM	21.219	74.291	41.890	14.095
CPM	12.037	38.695	22.469	7.360
FPM	4.113	52.497	19.422	10.687
CPM/IPM (%)	29.336	84.436	55.206	13.662
FPM/IPM (%)	15.564	70.664	44.794	13.662

**IPM** - Inhalable particle mass concentration (PM10); **CPM** - Coarse mode aerosol mass concentration (particles with diameters,  $2.5 < d_p < 10\mu\text{m}$ ); **FPM** - Fine mode aerosol mass concentration (particles with diameters,  $d_p < 2.5\mu\text{m}$ )

coarse mode. This can be due to emissions from sources such as sea spray (due to closeness of sampling station to the sea, about 600 m) and windblown dust (due to prevailing hamarttan weather conditions during sampling period) in the vicinity of the study location since coarse particles are predominantly emitted from the natural environment. On the other hand, it was observed that the range of FPM measured during the sampling period is much higher compared to that of the CPM. This probably indicates the relatively high levels of anthropogenic emissions particularly, those contributed from the source of livelihood activities in the community (mainly, fish smoking and fire woods) as well as vehicular traffic to atmospheric fine particle pollution in the Abuesi area. This is because, particles with aerodynamic diameter,  $dp < 2.5 \mu\text{m}$  occur mainly from anthropogenic sources (Panyacosit, 2000).

Although it is extremely difficult to compare aerosol concentrations measured either at different locations, or with different samplers, or at different periods with seasonal variations, the mean mass concentrations measured for both coarse and fine aerosol fractions in this study were much lower than that reported at Ashaiman (a suburban town in Ghana) by Ofosu et al. (2009) for CPM ( $109.56 \mu\text{g}/\text{m}^3$ ) and FPM ( $23.95 \mu\text{g}/\text{m}^3$ ). The difference is largely attributed to the fact that, unlike Abuesi, Ashaiman is densely populated and characterised by heavy vehicular traffic. Also, the closeness of Ashaiman to Tema (a heavily industrialised city in Ghana) means ambient air in the vicinity is largely affected by transport of these industrial emissions.

**Table 4.2: International Air Quality Standards and Guidelines**

Particulate Size	Time	Ambient Air Quality Standards in $\mu\text{g}/\text{m}^3$			
		US-EPA	WHO	EU	GHANA-EPA
PM10	Annual	50	20	40	N/A
	24hr	150	50	50	70
PM2.5	Annual	15	10	25	N/A
	24hr	35	25	N/A	N/A

It can be seen from table 4.2, that the WHO has a 24 hr standard of  $50 \mu\text{g}/\text{m}^3$  and  $25 \mu\text{g}/\text{m}^3$  for PM10 and PM2.5 respectively. However, comparison of the WHO standard values with the obtained IPM arithmetic means for the Abuesi area (i.e.,  $41.890 \mu\text{g}/\text{m}^3$  for PM10 and  $19.422 \mu\text{g}/\text{m}^3$  for PM2.5) indicates that the PM10 in the study area is lower and, therefore, does not pose any threats of exposure of the inhabitants to severe health risks. The rather low values could be attributed to the climatology (strong winds resuspended dust causing elevated dust levels and occasional rainfalls) of the Abuesi area. Nevertheless, the risk for various outcomes has been shown to increase with exposure and there is also little evidence for a threshold below which no adverse health effects would be anticipated. Hence, there is the need to regulate the level of atmospheric fine particle pollution in the area.

The time series of the coarse and fine mass concentrations for the Abuesi sampling site is as indicated in Figures 4.1, 4.2 and 4.3. The relatively high variability observed, with PM10 mass concentrations varying from  $21.219 \mu\text{g}/\text{m}^3$  to  $74.291 \mu\text{g}/\text{m}^3$  could be due to variations in weather conditions as well as daily human activities at the sampling site.

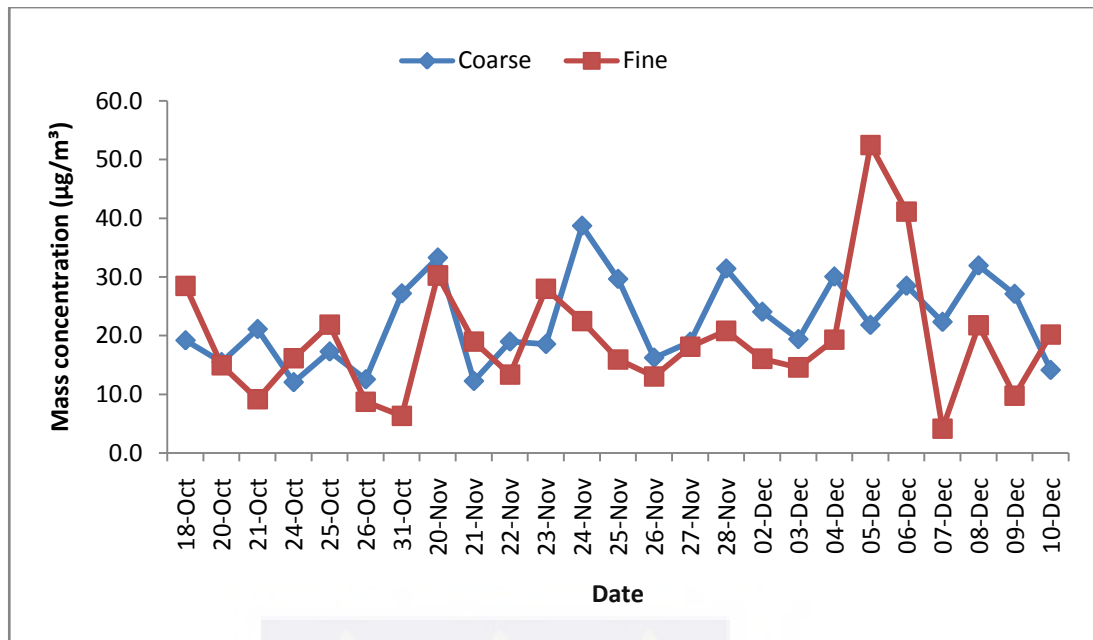


*Fig. 4.1: Aerosol mass concentrations for daily measurements for both fine and coarse components of IPM at Abuesi*

From Fig.4.2, the highest and lowest mean values for the CPM were recorded on Saturday and Monday respectively, whilst that for the FPM was Thursday and Sunday respectively. The study area is predominantly an Adventist community and, therefore, the high CPM mean value recorded on Saturday reasonably affirms the notion that there is little or no fish smoking activities (the main source of anthropogenic emission in the area) due to observation of the Sabbath. Thus, a large fraction of the suspended particulate collected fell within the coarse mode.



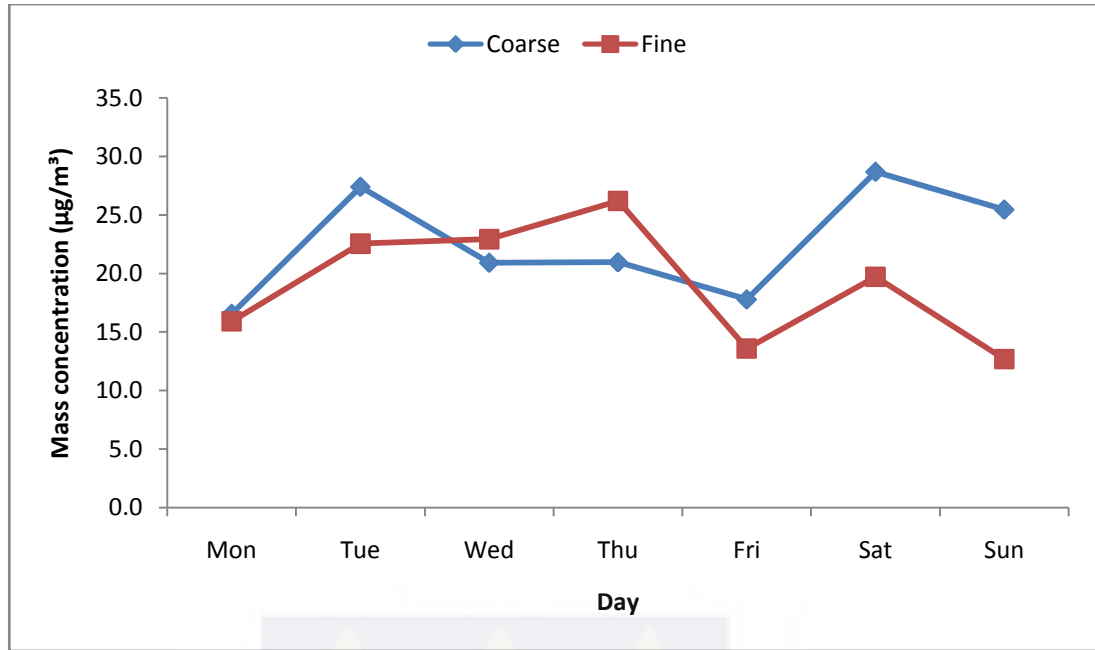


*Fig. 4.2: Variation of average CPM and FPM concentrations for days of the week during the sampling period*

The observed linearity in Fig. 4.3, for both CPM and FPM is representative of the gradual increase in saturation levels of airborne particulates pollution episodes due to prevailing harmatan dust over the three months sampling period (i.e., October to December). This was evident in all scenarios, with mean CPM values higher than that of the FPM. However, the rise in mean FPM values between November and December (i.e., 20.089  $\mu\text{g}/\text{m}^3$  - 22.145  $\mu\text{g}/\text{m}^3$ ; about 4.9 %) was significantly higher compared to that of the CPM (i.e., 24.207  $\mu\text{g}/\text{m}^3$  - 24.348  $\mu\text{g}/\text{m}^3$ ; about 0.3 %) in the same period. This could be due to increase in fish smoking activities in the community ahead of the Christmas festive season.

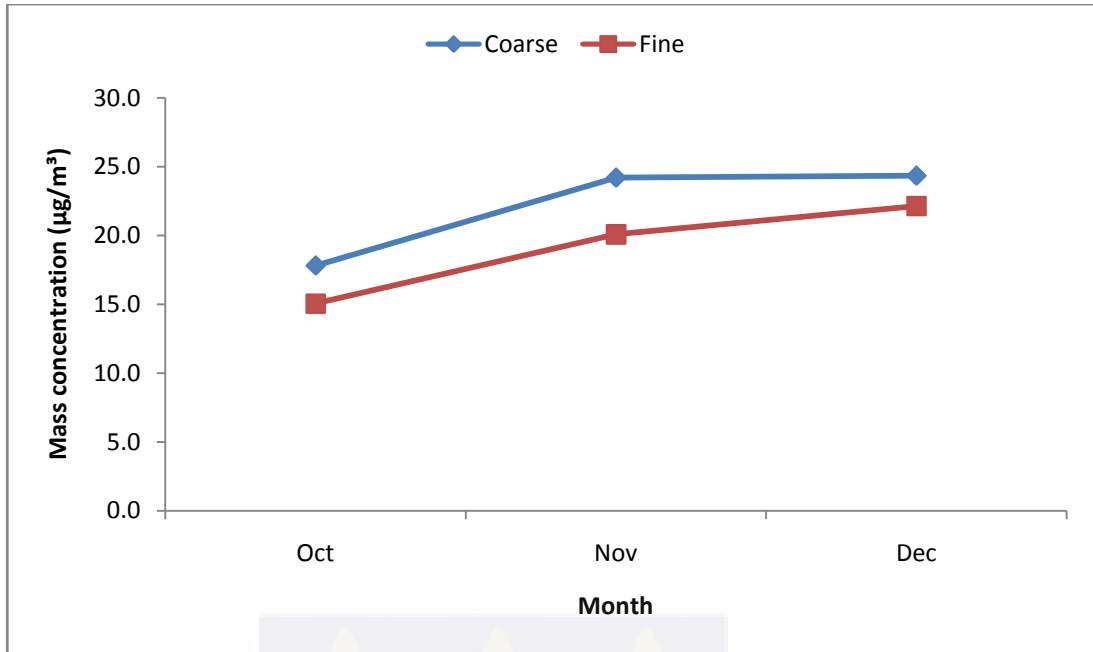


Fig. 4.3: Variation of average CPM and FPM for the three months sampling period

#### 4.2 Elemental Analysis

Figure 4.4 shows a typical fitted spectrum of air filter sample analyzed using EDXRF.

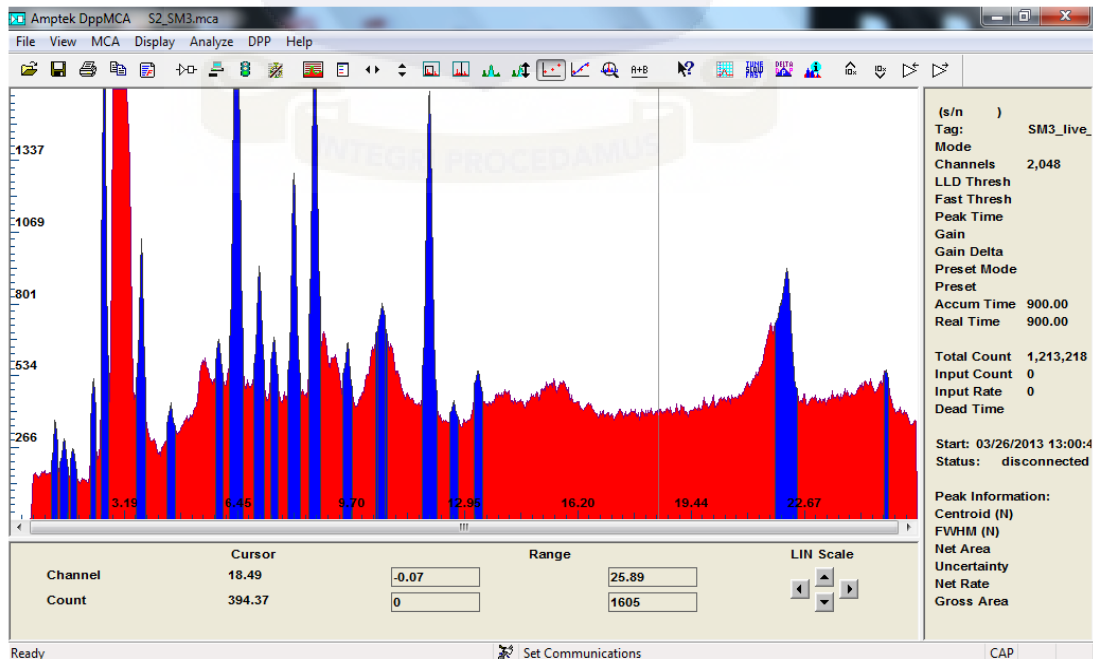


Figure 4.4: Typical fitted spectrum of loaded coarse air filter sample using EDXRF

The area under each peak corresponds to an unknown concentration of an element of interest and is indicated by the blue regions. To determine the actual concentrations of the measured elements, the yield (net count per second per milliamper) recorded for each element was employed using equation (3.4).

The range of measured elemental abundances for 28 elements in ambient air at Abuesi is presented in Table 3.10 (see appendices). Some environmentally important elements including Na, Mg, Al, K, Ca, Cr, Mn, Fe, Cu, Zn, Br, Pb and Cd are listed. Figure 4.5 reveals that Abuesi's aerosol is rich in chlorine, Cl, recording the highest average concentration value of  $1.916 \mu\text{g}/\text{m}^3$ .

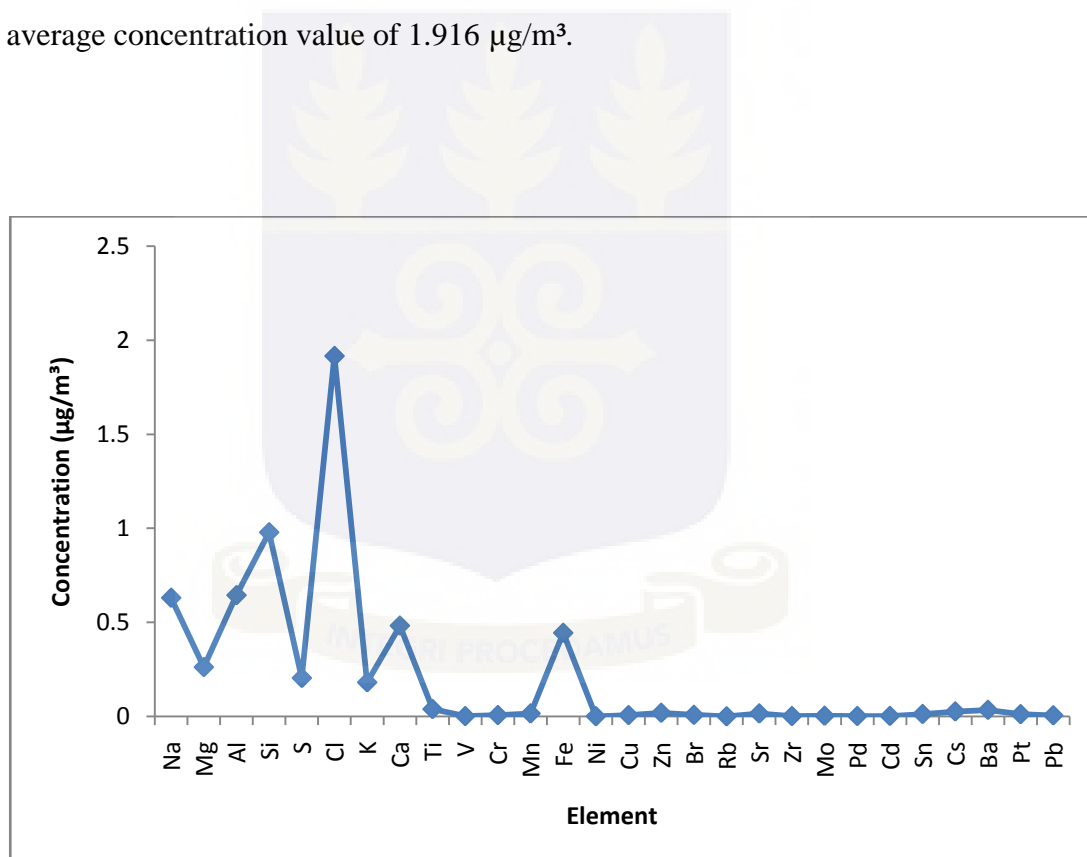


Figure 4.5: Average coarse mode aerosol elemental concentrations ( $\mu\text{g}/\text{m}^3$ ) from Abuesi

#### **4.2.1 Treatment**

It may be argued that ambient air of the Abuesi area is generally clean due to the absence of industrialized activities. Also, coarse particles accounted for about 54% of the total mass of IPM collected. This suggests that sources of aerosols in the vicinity are mainly limited to crustal material/dust and sea spray with relative contributions of trace amounts from other anthropogenic sources including smoke from combustion activities, transport and long range transport of industrial emissions from thermal plants at Aboadze. Of all the 28 measured elements, only Na, Mg, Al, Si, S, Cl, K, Ca and Fe recorded a relatively significant average elemental concentration values. These elements are known to predominantly originate from the natural environment and thus, reaffirm the concept that the bulk majority of APM in the Abuesi area is contributed by natural sources.

#### **4.2.2 Na, Cl, S, K and Ca**

The main contributor of sodium in aerosols is sea spray and its distribution is influenced by the strong southerly winds and the topography of the Abuesi area. The relatively high level of Na recorded is an indication of the closeness of the sampling station (about 100 m) to the sea which is made up of water and salt (NaCl). Also, sea spray predominantly consists of coarse particles with relatively small residence time in the atmosphere, hence the detection of Na in the coarse mode aerosol samples.

The observed high concentration of Cl is also attributed to sea spray aerosols because sea salt is particularly rich in NaCl. This is again indicative of the robust contribution of marine aerosols to the atmospheric fine particle pollution at Abuesi.

According to Shaw (1983) and Charlson et al. (1987), sulphur species have been historically thought to be the primary chemical component in secondary marine aerosol production, originating predominantly from the oxidation of SO<sub>2</sub>. Thus, it is not surprising to observe some relative contributions of sulphur to the measured coarse mode aerosols. Sulphur can as well be emitted from combustion processes at Aboadze thermal plants due to the presence of sulphur compounds in crude oil (which serves as fuel for the thermal plants).

Although potassium can be derived from marine and/or crustal material, its mean concentration value of 0.181 µg/m<sup>3</sup> recorded for Abuesi coarse mode aerosol could strongly be argued to originate partly from biomass burning due to the enormous fish smoking activities (primary source of livelihood) in the community.

Resuspended dust is the main contributor of Ca to the coarse mode aerosol at Abuesi, although long range transport of dust particles from the Sahara desert cannot be ruled out due to the prevalence of harmattan weather conditions during the sampling period.

#### **4.2.3 Al, Si, Mn and Fe**

Aluminum is known to be the most abundant metal and the third most abundant element in the earth's crust, comprising about 8.8 % by weight. According to Lantzy and MacKenzie (1979), due to its prominence as a major constituent of the earth's crust, contributions from natural weathering processes to APM far exceeds releases into the atmosphere by anthropogenic emissions. Thus, the 0.644 µg/m<sup>3</sup> of Al measured in the coarse mode are predominantly of crustal origin.

Silicon also originates predominantly from the earth crusts in the form of quartz. Thus, the recorded mean value of 0.979 µg/m<sup>3</sup> in the coarse mode could as well be

conveniently attributed to crustal sources although some relatively small contributions from anthropogenic activities cannot be ruled out.

According to ATSDR (2000), natural sources of manganese to the atmosphere are the result of the erosion of soils and dusts whereas anthropogenic sources occur mainly from industrial activities (such as alloy production and steel foundries) and combustion of fossil fuels (in power plants, coke ovens and automobiles, for example). Since Abuesi is free from any immediate exposure to industrial pollution sources, the mean value of  $0.016 \mu\text{g}/\text{m}^3$  recorded for Mn could be contributions from resuspended dust particles.

At Abuesi, it is expected that contributions of biomass burning with its attendant particulates will be high due to the prevailing fish smoking activities in the community. However, Chen et al. (2007) and Lee et al. (2005) have reported that total Fe concentrations in biomass burning emissions typically account for less than 1 % of total burnt emissions suggesting the mean value of  $0.444 \mu\text{g}/\text{m}^3$  recorded at Abuesi were most likely of crustal material/dust origin.

#### **4.2.4 Cr, Cu, Zn, Br and Pb**

The average chromium level in coarse mode aerosol at Abuesi was found to be about  $0.007 \mu\text{g}/\text{m}^3$ . According to the US EPA (2003), continuous exposure to IPM containing  $0.0008 \mu\text{g}/\text{m}^3$  (equivalent of  $0.8 \text{ ng}/\text{m}^3$ ) of Cr would result in less than a one-in-a-hundred thousand increased risk of developing cancer in one's lifetime. Trace amounts of chromium in Abuesi's ambient air could be due to emissions from industrial activities at Aboadze thermal plants.

A mean value of  $0.007 \mu\text{g}/\text{m}^3$  was also recorded by copper. This is well in agreement with Davies and Bennet (1985) who noted that average levels of Cu in ambient air are usually less than  $1 \mu\text{g}/\text{m}^3$  except for urban or highly polluted areas. The presence of this trace amount, however, could be contributions from vehicular emissions and other anthropogenic sources.

The presence of Zn in Abuesi's aerosol could be attributed to contributions from the wear-off of automobile tyres and brake pads since Zn is used in their manufacture (Kennedy and Gadd, 2003) as well as emissions from vehicular exhaust. An average value of  $0.019 \mu\text{g}/\text{m}^3$  was recorded as the elemental contribution of Zn to the fine particle pollution of the study area.

According to Ganley and Springer (1974), motor vehicular emissions in the form of lead halides are the main source of bromine, Br, in aerosols. Again, Martens et al. (1973) argues that some Br content in APM is contributed by marine aerosols. However, these contributions do not account for more than 5 % of total Br even at sea side locations. The average value of  $0.008 \mu\text{g}/\text{m}^3$  recorded could most likely originate from marine aerosol because Br from the sea dominates in the coarse mode at sea side locations.

The WHO guideline for Pb is  $0.5 \mu\text{g}/\text{m}^3$  per annum. This value is far greater than the  $0.006 \mu\text{g}/\text{m}^3$  registered at Abuesi. With the absence of Pb fuelled vehicles, sources of Pb in the coarse mode aerosol at Abuesi could be attributed to resuspended soil dust.

Generally, the presence of these heavy metals in the coarse mode aerosols indicates a rather robust blend of sea spray and resuspended soil dust in the Abuesi area with

contributions from combustion and other anthropogenic sources as far as atmospheric fine particle pollution in the area is concerned.

### 4.3 Multivariate Receptor Model

#### 4.3.1 Cluster Analysis

Application of HCA to the EDXRF data helped to reduce the complex multivariate data to smaller subsets or groups based on their similarity.

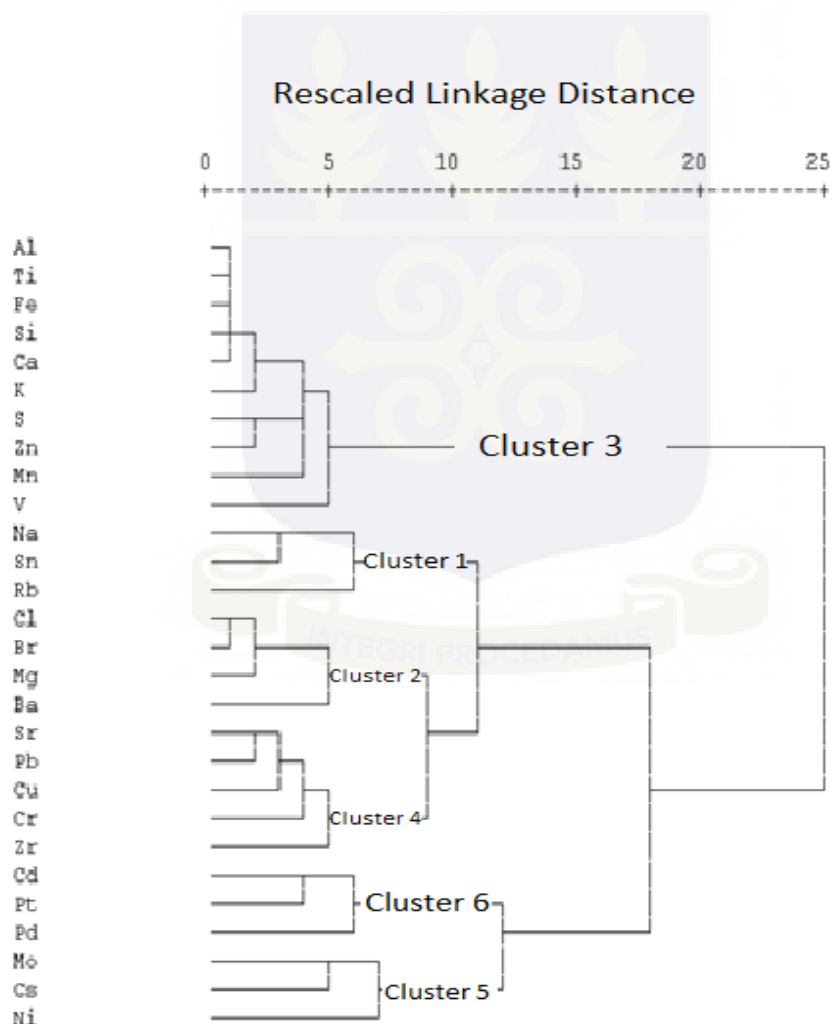


Figure 4.6(a): Dendrogram from HCA showing the distribution of elements in the coarse mode aerosols



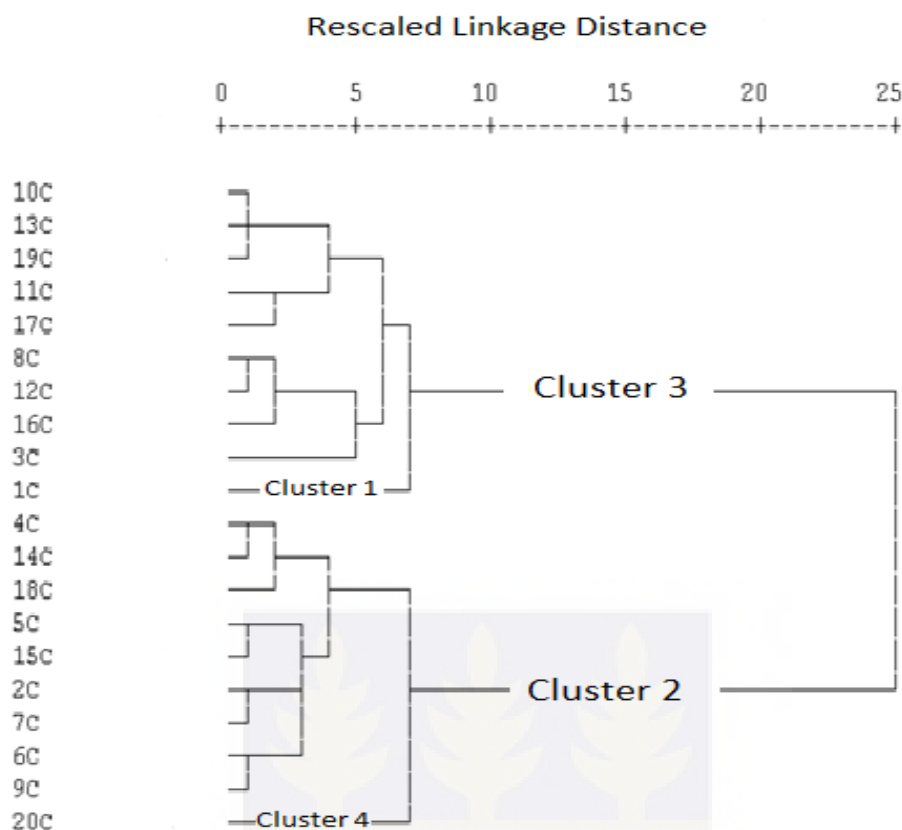


Figure 4.6(b): Dendrogram from HCA showing the distribution of daily coarse aerosol samples collected

Figure 4.6 (a, b) represents dendrograms acquired from the Euclidean distances (the simplest distance measured between two objects) using the Ward's linkage method.

A total of six clusters out of a major two were observed from Figure 4.6(a) in the Cluster analysis. This agrees in principle with the two major sources of APM to the aerosol problem globally (i.e., natural and anthropogenic sources). Clusters one, five and six contained three elements each and were respectively represented by Na, Sn, Rb; Mo, Cs, Ni and Cd, Pt, Pd. Magnesium, Cl, Br and Ba constituted cluster two whilst cluster four was constituted by Cr, Cu, Sr, Zr and Pb. Cluster three was found to contain a total of 10 elements including Al, Si, S, K, Ca, Ti, V, Mn, Fe and Zn which accounted for about 35.71 % of the bulk of the measured elements. These

elements are known to predominantly originate from crustal material and thus a cluster grouping of this sort was expected. The various cluster groupings, typically, indicates a similarity in activities of emission sources contributing to the APM in the Abuesi area.

Similarly, Figure 4.6(b) yielded two major clusters out of a possible four. However, the rather robust sub clustering observed here indicates possible fluctuations in experimental conditions and/or variations due o changing weather conditions and human activities from one day to another. This is well in agreement with the relatively high variability observed in the time series (TSPM mass concentration distribution) in Figure 1 during the entire sampling period. According to cluster memberships from the HCA, clusters one and four were found to contain one case each (i.e., 1C and 20C respectively). Similarly, 9 cases each constituted clusters two and three with samples 2C, 4C, 5C, 6C, 7C, 9C, 14C, 15C and 18C forming cluster two whilst samples 3C, 8C, 10C, 11C, 12C, 13C, 16C, 17C and 19C constituted cluster three. Also, about 67 % of the aerosol samples constituting cluster two were collected on weekdays whilst 56 % were collected on weekends in cluster three (see Table 3.1). These cluster groupings primarily indicate a similar mass loading of APM collected during sampling. Furthermore, this could largely be due to collected aerosol samples originating from similar activities in separate instances per each day of the sampling period.

## 4.3.2 Principal Component Analysis (PCA)

**Table 4.3: VARIMAX rotated factor loading matrix of the coarse mode aerosol for Abuesi**

Element	PC 1	PC 2	PC 3	PC 4	PC 5	PC 6
Na	-0.112	0.460	0.433	0.482	-0.334	0.099
Mg	0.115	0.892	0.231	-0.049	-0.186	-0.003
Al	0.976	0.108	0.042	0.009	0.004	-0.053
Si	0.979	0.056	0.000	0.020	-0.039	-0.070
S	0.718	0.552	-0.073	-0.162	-0.172	0.031
Cl	0.545	0.720	0.064	0.245	-0.013	-0.025
K	0.821	0.265	0.043	0.179	-0.183	-0.103
Ca	0.939	0.147	0.091	-0.095	-0.120	0.044
Ti	0.981	0.097	0.068	-0.024	-0.012	-0.045
V	0.655	-0.228	0.222	-0.014	0.231	-0.301
Cr	0.234	0.049	0.889	-0.026	0.000	0.124
Mn	0.745	0.217	-0.069	0.342	0.279	0.272
Fe	0.983	0.101	0.022	0.042	-0.010	-0.010
Ni	0.092	-0.124	-0.837	-0.254	-0.214	0.225
Cu	0.191	0.706	0.434	0.180	0.148	0.132
Zn	0.691	0.555	0.147	0.091	0.122	-0.013
Br	0.343	0.894	-0.020	0.004	-0.054	-0.086
Rb	0.136	0.027	-0.046	0.770	0.049	-0.119
Sr	0.541	0.507	0.423	-0.216	0.040	-0.081
Zr	0.507	0.397	0.099	-0.377	0.206	-0.022
Mo	-0.083	-0.108	-0.048	-0.248	-0.229	0.677
Pd	0.046	-0.115	0.073	0.169	0.585	-0.273
Cd	-0.109	-0.075	0.002	-0.143	0.886	0.016
Sn	0.015	0.201	0.342	0.671	-0.047	0.165
Cs	-0.133	-0.080	0.061	0.412	0.104	0.740
Ba	-0.152	0.668	-0.217	0.329	-0.009	-0.200
Pt	-0.031	0.343	0.422	-0.042	0.619	0.361
Pb	0.406	0.547	0.392	-0.035	0.190	0.415
Eigen Value	8.711	5.035	2.721	2.212	2.102	1.761
Variance (%)	31.111	17.983	9.717	7.901	7.506	6.289

\* The total variance explained by the 6 retained factors in Abuesi is 80.508% of the original data variability

As discussed earlier, identification of pollutant sources was accomplished by PCA with VARIMAX rotation on the elemental concentrations. The number of factors retained in this work was determined by the scree test (Cattell, 1996). The result is as reported in Table 4.3. Also presented are the percentage variances explained by each of the factors as well as their respective eigen values. The six principal

components accounted for 80.51 % of the total variance in the data set (i.e., PC 1, PC 2, PC 3, PC 4, PC 5 and PC 6 accounted for 31.11 %, 17.98 %, 9.72 %, 7.90 %, 7.51 % and 6.29 % respectively). The observed percentage variances indicate the relative contributions of each component with factors one and two recording significantly higher variances than the other four factors.

The values in this matrix represent the relations between each variable as well as each of the six retained factors. From their composition, three main sources were identified including crustal material/soil dust, marine (sea spray) and mechanical operations (anthropogenic sources).

The first factor represents crustal material (resuspended dust) mixed with smoke. This factor recorded high loadings for about 46.43 % of the measured elements with Al, Si, K, Ca, Ti, Mn, Fe and Zn constituting emissions from crustal material/dust whilst S, Cl, V, Sr and Zr constitute smoke particularly wood burning and refuse incineration. These mixtures on the same factors indicate that the coarse mode aerosol observed at Abuesi is a very mixed component.

Similarly, PC 2 contains high loadings for elements representing a mix of marine (sea spray) to the aerosol problem in Abuesi. Magnesium, S, Cl, Br and Sr are major elemental markers attributed to sea spray aerosol whilst transport emissions are associated to Cu, Zn, Ba and Pb. It is important, however, to note that these transport emissions are predominantly non-exhaust, including tyre wear, brake wear, road surface wear and the corrosion of other vehicular components among others. For instance, the source of Pb is not likely to be leaded petrol since lead in petrol has been phased out in Ghana. However, unleaded oil fuels may still contain trace amounts of lead which may originate from crude oil. According to Sternbeck et al.

(2002), brake wear is a major emission pathway for Cu and Ba. The corrosion of vehicle components can as well contribute to the deposited dust on road surface and hence forms part of resuspended material. Regarding this, Harrison et al. (2001) concluded that vehicle-induced resuspension has source strength approximately equal to that of exhaust emissions.

Factor 3 (PC 3) contained high loading for only Cr. According to Pacyna and Pacyna (2001), Cr is released into the atmosphere mainly by anthropogenic stationary point sources, including industrial, commercial, and residential fuel combustion, via the combustion of natural gas, oil, and coal. Other potentially small sources of atmospheric chromium emission includes cement-producing plants, incineration of municipal refuse and sewage sludge, emission from chromium-based automotive catalytic converters among others. Thus, the presence of Cr could be releases from mechanical operations. Again, Cohen et al. (2002) reported Ni as a major elemental marker for industrial emissions. Thus, the strong negative correlation observed in PC 3 between Cr and Ni suggests that total Cr in the coarse mode Abuesi aerosol could contain some relative contributions from other anthropogenic sources including sewage incineration and non-vehicular exhaust.

Rubidium and Sn also registered high loadings for PC 4. This unusual chemical grouping is attributed to non-vehicular exhaust (Sn). Some support for this assertion is provided by Kennedy and Gadd (2000) who reported elevated concentration levels of Sn among other metals in their assessment of trace heavy metals in butimen milled from the road surface after a period of vehicular movement on the road surface.

PC 5 is attributed to platinum group metals with high factor loadings for Pt and Pd. There is also an unusual association with Cd, also recording a high factor loading. This group of elements occurs in trace quantities and is known to predominantly originate from non-vehicular exhaust due to their use as catalysts in automotive catalytic converters. According to Avino et al. (2008), the dominant fraction of airborne Cd generally comes from anthropogenic processes such as fossil fuel combustion, the operation of waste incinerators and power plants. In contrast, Hieu and Lee (2010) classified terrestrial dust, wild fires and volcanic emissions as the main sources of natural Cd. However, Cd association with the Pt group metals can possibly be contributions from anthropogenic sources with emissions from combustion processes at Aboadze thermal plants being dominant since crude oil contains trace amounts of Cd.

Factor 6 (PC 6) showed high loadings for Mo and Cs. In a study by Kennedy and Gadd (2000), Mo was reported as one of the elements with elevated concentration levels in road butimen after investigations of trace heavy metals in portions of milled butimen from road surface in New Zealand. The association of Cs to Mo in this factor is not readily accounted for although Cs is commonly known to originate from crustal rich sources.

Sodium showed an approximate even size distribution in PC 2, PC 3 and PC 4 suggestive of having multiple sources. In PC 2, Na could conveniently be attributed to sea spray aerosols due to the richness of sea water in common salt (NaCl). In PC 3, Na could result from industrial emission from Aboadze thermal plant due to its association with Cr. This is because crude oil used as fuel for the thermal plants contains significant amounts of inorganic salts including NaCl, thus leaving the possibility of trace amounts of Na being released from the combustion process. The

association of Na with Rb and Sn in PC 4 is rather unusual and not readily accounted for in this present work. Also, four elements including S, Cl, Zn and Sr registered high factor loadings on both PC 1 and PC 2 indicating the possibility of a multiple source for their presence in the coarse mode Abuesi aerosol. Table 4.4 shows a summary of APM sources and their elemental markers for the Abuesi area.

Figure 4.7 shows a plot of the principal components for elemental groupings obtained from the PCA. The elemental groupings typically reflect the contributions from various sources to the atmospheric fine particle pollution in the Abuesi area. The second quadrant of the plot consisted of all the elements associated with PC 1 and PC 2. These two moderately mixed clusters of elements constituted emissions from dust/crustal material, smoke, sea spray and transport and largely represented the bulk of APM sources in the Abuesi area. This plot sheds more light on the dendrogram (Figure 4.6) which showed the distribution of elements associated with the coarse mode aerosols.

**Table 4.4: Elemental markers associated with the APM sources in the Abuesi area as determined by the PCA**

Crustal Material/Dust	Al, Si, K, Ca, Ti, Mn, Fe, Zn
Marine (sea spray)	Na, Mg, S, Cl, Br, Sr, Sn, Pt
Anthropogenic sources	Cu, Zn, Ba, Pb, S, Cl, Br, V, Sr, Zr Cr, Cd, Mo, Cs, Sn, Pd, Rb, Pt, Na

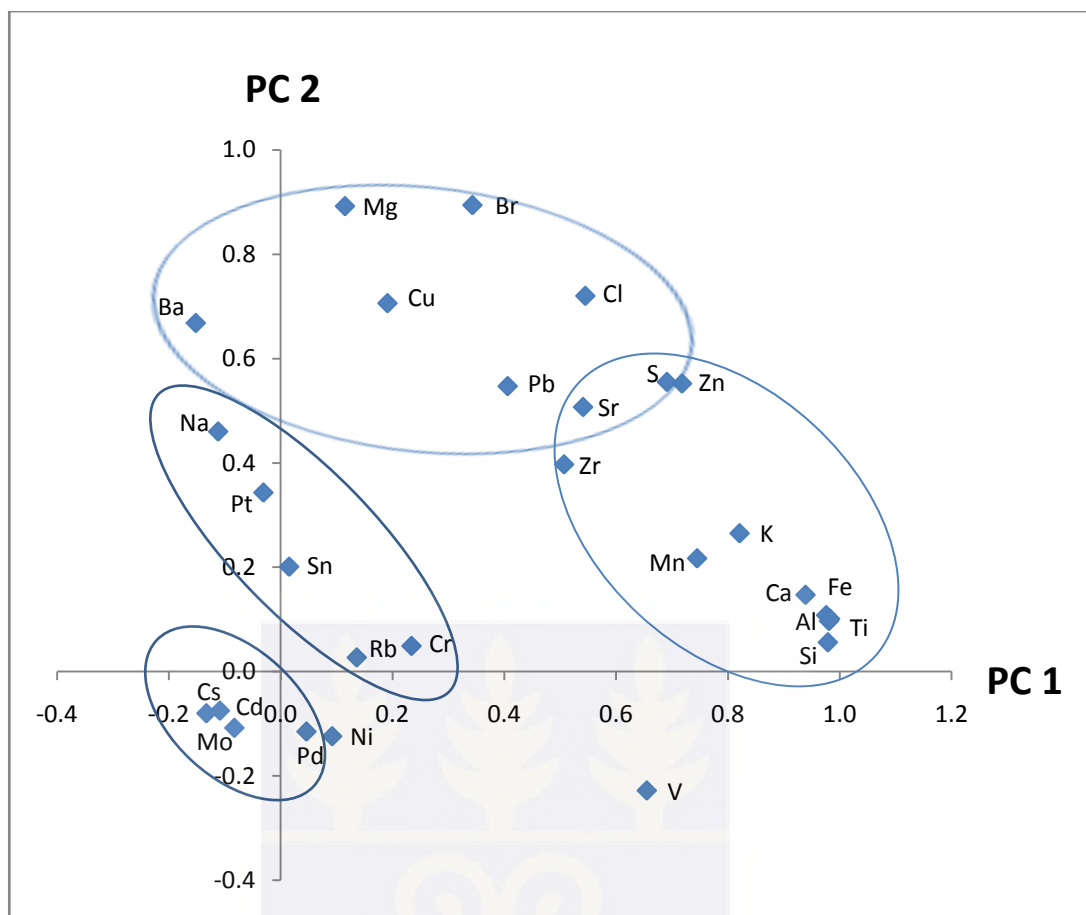


Figure 4.7: Plot of principal components of elements in the coarse mode aerosols from Abuesi area

#### 4.4 Enrichment Factors

Figure 4.8 presents the EF values for the coarse mode aerosols sampled in the Abuesi area. About 14 % of the detected elements including Na, Mg, K and Ca recorded some degree of enrichment. Sodium had the highest EF value of 3.386, indicating moderate enrichment. This largely reflects the level of marine aerosol (sea spray) contribution to the APM in the Abuesi community.



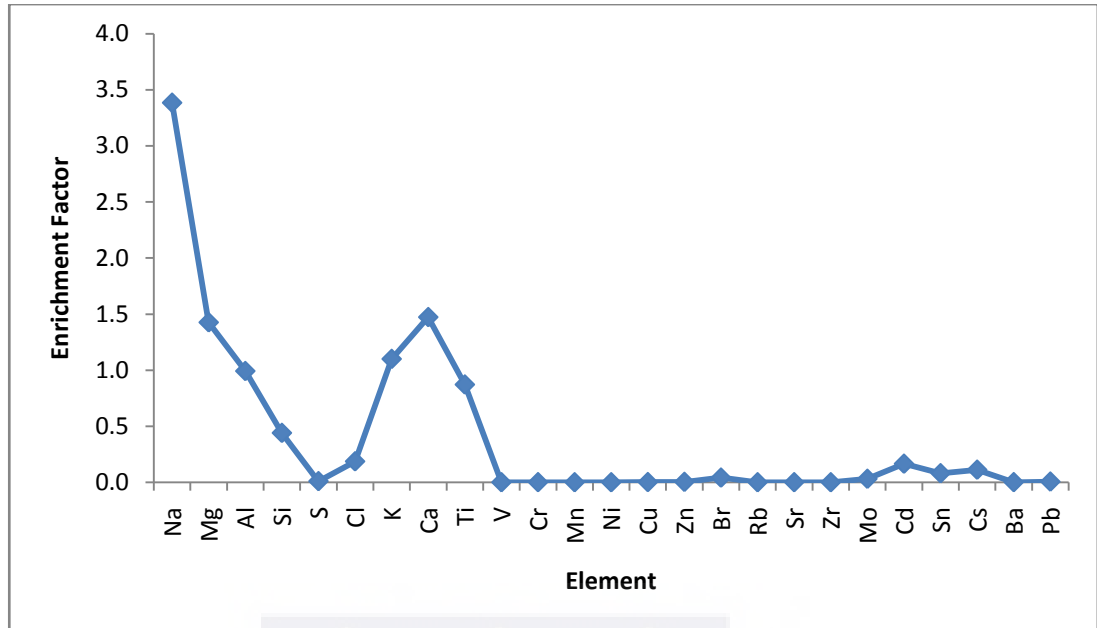


Figure 4.8 Enrichment Factor (EF) values calculated for coarse mode aerosol samples

An observation of Figure 4.8 shows that some elements (Na, Mg, K, Ca) have EF values  $>1$ , indicating their origin from possibly same source (i.e. crustal and marine). A second group (Al, Ti, Si) which generally have crustal material/dust as their main source of origin have EF values near 1. Finally, all the other elements recorded EF values approximately zero, indicating no enrichment at all. These elements represent a mix of natural and anthropogenic APM sources in the Abuesi area. The very low EF of elements from V to Pb shows that contribution of anthropogenic particulates to the particulate loadings in the coarse mode is not significant.

## CHAPTER FIVE

### CONCLUSION AND RECOMMENDATION

#### 5.1 Conclusions

A total of 25 aerosol samples were collected in the Abuesi area using a Gent sampler with Nuclepore filters, over a period of approximately three months. Mean values measured for IPM (PM<sub>10</sub>), CPM and FPM were 41.890  $\mu\text{g}/\text{m}^3$ , 22.469  $\mu\text{g}/\text{m}^3$  and 19.422  $\mu\text{g}/\text{m}^3$  respectively. These values are much lower than WHO standards and thus, suggest the “safeness” of ambient air in the study area. Both the CPM and FPM accounted for 29.34 % and 15.56 % respectively of IPM collected. Time series plots also revealed a relatively high variability for PM<sub>10</sub> mass concentrations due to changing weather conditions and human activities from time to time with a continuous rise in saturation levels of APM over the sampling period.

A total of 28 elements including heavy metals were measured by EDXRF experiment in the coarse mode aerosol samples. Amongst the elements, Cl, recorded the highest average concentration value of 1.916  $\mu\text{g}/\text{m}^3$  indicating the immense contribution of sea spray to the aerosol situation at Abuesi. The elements Na, Mg, Al, Si, S, Cl, K, Ca and Fe recorded a relatively significant average elemental concentration values. These elements originate predominantly from natural sources and, thus, it is concluded that the bulk majority of APM in the area originates from the natural environment. The presence of heavy metals also denotes contributions from transport and industrial emissions as well as other anthropogenic sources to the atmospheric aerosol problem in the area. Generally, the recorded mean elemental concentrations were found to be lower than the WHO guideline values.

Multivariate statistical analysis helped to identify crustal material (resuspended dust), smoke, marine (sea spray), transport and industrial emissions as the main sources of APM at Abuesi. Six major elemental groupings were first observed from the cluster analysis which represented six different sources (with three main) APM sources in the area as determined by the PCA. Also, the PCA with VARIMAX rotation yielded six factors score which accounted for 80.51 % of the original data variability and as well, agreed with the three identified sources contributing to the fine particle pollution in the Abuesi area.

The “safeness” of Abuesi’s ambient air was further supported by the fact that about 86 % of the measured elements recorded no enrichment at all (i.e.  $EF < 1$ ) with the remaining 14 % registering depletion to minimal enrichment to moderate enrichment. Also, the highest EF value recorded by Na is indicative of the degree of marine aerosol contribution to the APM in the study area. In conclusion, no significant degree of contamination of APM by the measured elements in the coarse mode aerosol content of the Abuesi area was recorded.

## 5.2 Recommendation

It is recommended that further studies be conducted, preferably long term monitoring of the area to:

- i. Estimate the black carbon and elemental concentrations of both fine and coarse aerosol fractions.
- ii. Conduct source apportionment to quantify the relative elemental source profile of the various APM sources in the area.
- iii. Assess the health risk of the atmospheric aerosol situation in the area.
- iv. Develop a model to describe the aerosol problem in the area.

## REFERENCES

Abdi H. (2003). Multivariate analysis. In M. Lewis-Beck, A. Bryman, and T. Futing (Eds), Encyclopedia for research methods for the social sciences. Thousand Oaks, CA: Sage.

Agency for Toxic Substances and Disease Registry (1999). Toxicological profile for lead, Atlanta, GA: US Department of Health and Human Services.

Akoto Bamford S., Wegrzynek D., Chinea-Cano E. and Markowicz A. (2004). Application of X-ray fluorescence techniques for the determination of hazardous and essential trace elements in environmental and biological materials. NUKLEONIKA: 49(3):87-95.

Almeida S.M., Freitas M.C., Reis M.A., Pio C.A. and Trancoso M.A. (2006). Combined application of multielemental analysis –  $k_0$ -INAA and PIXE – and classical techniques for source apportionment in aerosol studies. Nuclear Instrument and Methods in Physics Research, A 564, 752-760.

Artaxo P., Oyola P. and Martinez R. (1999). Aerosol composition and source apportionment in Santiago de Chile. Nuclear Instruments and Methods in Physics Research B 150, 409-416.

Avino P., Capannesi G. and Rosada G. (2008). Heavy metal determination in atmospheric particulate matter by Instrumental Neutron Activation Analysis. Microchem. J. 88: 97-106.

Baptista Neto J.A., Smith B. J. and McAllister J.J. (2000). Heavy metal concentrations in surface sediments in a near shore environment, Jurujuba Sound, Southeast Brazil. Environ. Pollut., 109 (1), 1-9.

Begum B.A., Biswas S.K., Markwitz A. and Hopke P.K. (2010). Identification of Sources of Fine and Coarse Particulate Matter in Dhaka, Bangladesh. Aerosol and Air Quality Research, 10: 345–353.

Boamponsem L.K., Adam J.I., Dampare S.B., Nyarko B.J.B. and Essumang D.K. (2010). Assessment of atmospheric heavy metal deposition in the Tarkwa gold mining area of Ghana using epiphytic lichens. Nuclear Instruments and Methods in Physics Research, B. Vol. 268, 1492-1501.

Bogen J. (1973). Trace elements in atmospheric aerosol in the Heidelberg area, measured by instrumental neutron activation analysis. Atmospheric Environment 7, 1117-1125.

Brasseur G.P. and Roeckner E. (2005). Impact of improved air quality on the future evolution of climate. Geophys. Res. Lett., 32, L23704, doi:10.1029/2005GL023902.

Capes J.G., Murphy C.E., Reaves J.B., McQuaid J.F. and Hamilton J.R. (2009). Secondary organic aerosol from Biogenic VOCs over West Africa during African monsoon multidisciplinary analysis (AMMA). *Atmospheric Chemistry and Physics* 9, pp. 3841–3850.

Cattell R.B. (1996). The scree test for the number of factors. *Multivariate Behav Res* 1:245–276.

Charlson, R.J., Lovelock, J.E., Andreae, M.O. and Warren, S.G. (1987). Oceanic phytoplankton, atmospheric sulphur, cloud albedo and climate. *Nature* 326, 655 – 661. doi:10.1038/326655a0

Chen L.W., Moosmuller H., Arnott W.P., Chow J.C., Watson J.G., Susott R.A., Babbitt R.E., Wold C.E., Lincoln E.N. and Hao W.M. (2007). Emissions from laboratory combustion of wildland fuels: Emission factors and source profiles. *Environ. Sci. Technol.* 41 (12), 4317– 4325, doi:10.1021/es062364i.

Cohen D.D. (1998). Characterisation of atmospheric fine particles using IBA techniques. *Nuclear Instruments and Methods in Physics Research, B* 136-138, 14-22.

Cohen D.D., Stelcer E. and Garton D. (2002). Ion beam methods to determine trace heavy metals concentrations and sources in urban airsheds. *Nuclear Instruments and Methods in Physics Research, B* 190, 466-470.

Crutzen, P. J. (1998), Atmospheric aerosols: To the forefront of research in atmospheric chemistry. *IGBP, Global Change News Letter*, 33 : 9.

Daly A. and Zannetti P. (2007). Air pollution modeling – An overview. The Arab school for science and technology (ASST) and the EnviroComp Institute (<http://www.envirocomp.org>).

Dams R., Robins J.A., Rahn K.A. and Winchester J.W. (1970). Nondestructive neutron activation analysis of air pollution particulates. *Anal. Chem.*, 42, 861-867.

Deely J.M. and Ferguson J.E. (1994). Heavy metal and organic matter concentrations and distributions in dated sediments of a small estuary adjacent to a small urban area. *Sci. Total Environ.*, 153: 97-111.

Dentener F. et al., (2006). The global atmospheric environment for the next generation. *Environ. Sci. Technol.*, 40, 3586-3594.

Dotse S.Q., Asane J.K., Ofori F.G. and Aboh I.J.K. (2012). Particulate matter and black carbon concentration levels in Ashaiman, a semi-urban area of Ghana, 2008. *Research Journal of Environmental and Earth Sciences* 4(1):20-25. ISSN:2041-0492.

Duce R.A., Hoff G.L. and Zoller W.H. (1975). Atmospheric trace metals at remote northern and southern hemisphere sites: pollution or natural? *Science*, 187, 59-61.

Dzubay T.G. (1977). X-Ray Fluorescence Analysis of Environmental Samples, Ann Arbor Science, Ann Arbor, MI.

Fagbote E.O. and Olanipekun E.O. (2010). Evaluation of the Status of Heavy Metal Pollution of Soil and Plant (*Chromolaena odorata*) of Agbabu Bitumen Deposit Area, Nigeria. American-Eurasian Journal of Scientific Research 5 (4): 241-248, ISSN 1818-6785.

Ganley J.T. and Springer G.S. (1974). Physical and chemical characteristics of particulates in spark ignition exhaust. Environ. Sci. Technol. 8: 340-347.

Garimella S. and Deo R.N. (2007). Neutron activation analysis of atmospheric aerosols from a small pacific island country: a case of Suva, Fiji islands. Aerosol and air quality research, Vol.7, No.4, pp.500-517.

Hacsalihoglu G., Eliyakut F., Olmez I., Balkas T.I. and Tuncel G. (1992). Chemical composition of particles in the black sea atmosphere. Atmospheric Environment, 26A 3207-3218.

Hardin M. and Kahn R. (2010). Aerosol and climate change. NASA Earth Observatory Report.

Harman H.H. (1976). Modern factor analysis, Third Ed. Revised. University of Chicago Press, Chicago.

Harris F.S. (1976). Atmospheric aerosols: A literature summary of their physical characteristics and chemical composition. Old Dominion University, Norfolk, Va.23508, NASA Contractor Report, NASA CR-2626.

Haywood J.M. and Boucher .O (2000). Estimates of the direct and indirect radiative forcing due to tropospheric aerosols: A review, Rev. Geophys; 38, pp. 513-543.

Hieu N.T. and Lee B.K. (2010). Characteristics of particulate matter and metals in the ambient air from a residential area in the largest industrial city in Korea. Atmos. Res. 98: 526–537.

Hopke P.K. (1985). Receptor modeling in environmental chemistry. John Wiley, New York.

Hopke P.K., Xien Y., Raunemaa T., Biegalski S., Landsberger S., Maenhaut W., Artaxo P. and Cohen D. (1997). Characterization of the gent stacked filter unit PM10 sampler. Aerosol science and technology 27, 726-735.

Hopke P.K., Cohen D.D., Begum B.A., Biswas S.K., Ni B., Pandit G.G., Santoso M., Chung Y.S., Rahman S.A., Hamzah M.S., Davy P., Markwitz A., Waheed S., Siddique N., Santos F.L., Pabroa P.C., Seneviratne M.C., Wimolwattanapun W., Bunprapob S., Vuong T.B., Duy Hien P. and Markowicz A. (2008). Urban air quality in the Asian region. Science of the total environment 404: 103– 112.

[Http://www.who.org](http://www.who.org) (10<sup>th</sup> April, 2013)

[Http://www.usepa.org](http://www.usepa.org) (10<sup>th</sup> April, 2013)

[Http://www.ghanaepa.org](http://www.ghanaepa.org) (10<sup>th</sup> April, 2013)

[Http://www.eu.org](http://www.eu.org) (10<sup>th</sup> April, 2013)

[Http://www.horiba.com](http://www.horiba.com) (11<sup>th</sup> April, 2013)

Husar R.B. Atmospheric aerosol science before 1900. Centre for air pollution impact and trend analysis, Washington University, St. Louis, MO 63130.

Jackson J.E. (1991). A user's guide to principal components. New York: Wiley.

Jacobson, M.Z. (2001). Strong radiative heating due to the mixing state of black carbon in atmospheric aerosols. *Nature*, 409: 695–697.

Johansson S.A.E. and Johansson T.B. (1976). PIXE and its applications. *Nuclear Instruments and Methods in Physics Research*, 137, 473.

John W., Kaifer R., Rahn K. and Wesdowski J.J. (1973). Trace element concentration in aerosols from the San Francisco bay area. *Atmos. Environ.*, 7, 107-118.

Jolliffe I.T. (2002). *Principal component analysis*. New York: Springer.

Kaiser H.F. (1958). The varimax criterion for analytic rotation in factor analysis. *Psychometrika*, 23, 187(200).

Kennedy P. and Gadd J. (2003). Preliminary examination of trace elements in tyres, brake pads and road butimens in New Zealand. Research prepared by Kingett Mitchell Limited for New Zealand ministry of transport, November, 2000, revised in October, 2003.

Lee S., Baumann K., Schauer J.J., Sheesley R.J., Naeher L.P., Meinardi S., Blake D.R., Edgerton E.S., Russell A.G. and Clements M. (2005). Gaseous and particulate emissions from prescribed burning in Georgia. *Environ. Sci. Technol.*, 39 (23), 9049–9056, doi:10.1021/es051583l.

Loska K., Wiechula D. and Pelczar J. (2005). Application of enrichment factor to assessment of zinc enrichment/depletion in farming soils. *Commun. Soil Sci. Plant Anal.*, 36: 1117-1128.

Maenhaut W. (1992). The “Gent” stacked filter unit (SFU) sampler for the collection of atmospheric aerosols in two size fractions: description and instructions for installation and use, IAEA CRP E4.10.08, Belgium.

Maenhaut W., Salma I., Cafmeyer J., Annegam H.J. and Andreae M.O. (1996). Regional atmospheric aerosol composition and sources in the eastern transversal South Africa and impacts of biomass burning. *Journal of geophysical research*.

Martens C.S., Wesolowski J.J., Kaifer R. and John W. (1973). Pb and Br particle size distributions in the San Francisco Bay area. *Atmos. Environ.* 7: 905-914.

McCrone W.C. and Delly J.G. (1973). The particle atlas. Ed.2, Vol.1, Ann Arbor science publishers inc. Ann Arbor, MI.

Mucha A.P., Vasconcelos M.T.S.D. and Bordalo A.A. (2003). Macrobenthic community in the Doura estuary: Relations with trace metals and natural sediment characteristics. *Environ. Pollut.*, 121 (2), 169-180.

Mueller P.K. and Kothny E.L. (1973). Air pollution. *Anal. Chem.*, 45, 1R-9R.

Murley, L. (1991), Clean air around the world: National and international approaches to air pollution control. International Union of Air Pollution Prevention Associations (IUAPPA).

NAHRES-19, IAEA, Vienna (1994). Applied research on air pollution using nuclear-related analytical techniques. Report on the first research co-ordination meeting, Vienna, Austria, 30<sup>th</sup> March – 2<sup>nd</sup> April, 1993.

Ofori F.G., Hopke P.K., Aboh I.J.K. and Bamford S.A. (2012). Characterization of fine particulate sources at Ashaiman in Greater Accra, Ghana. *Atmospheric Pollution Research* 3, 301-310.

Ofori F.G., Hopke P.K., Aboh I.J.K. and Bamford S.A. (2013). Biomass burning contribution to ambient air particulate levels at Navrongo in the Savannah zone of Ghana. *Journal of the Air & Waste Management Association*, DOI: 10.1080/10962247.2013.783888

Ozba E.E. (2011). Heavy metals in surface soils of groves: A study from Istanbul, Turkey. *Scientific Research and Essays* Vol. 6(7), pp. 1667-1672. ISSN 1992-2248.

Paatero P. (1997). Least squares formulation of robust non-negative factor analysis, *Chemometr. Intell. Lab.*, 37, 23–35.

Pacyna J.M. and Pacyna E.G. (2001). An assessment of global and regional emissions of trace metals to the atmosphere from anthropogenic sources worldwide. *Environmental Reviews*, 9, 269-298. <http://dx.doi.org/10.1139/a01-012>.

Panyacosit L.(2000). A review of particulate matter and health: Focus on developing countries. International Institute for Applied Systems Analysis, IR-00-005.

Parr R.M., Stone S.F. and Zeisler R. (1996). Environmental protection: nuclear analytical techniques in air pollution monitoring and research. IAEA Co-ordinated Research Project. Volume 38, Issue No.2.

Pio C.A., Castro L.M. and Ramos M.O. (1993). Proceedings of the sixth European symposium on physical-chemical behavior of atmospheric pollutants.

Pope C.A., Burnett R.T., Thun M.J., Calle E.E., Krewski D., Ito K. and Thurston G.D. (2002), Lung Cancer, Cardiopulmonary Mortality, and Long-term Exposure to Fine Particulate Air Pollution, *Journal of the American Medical Association*, 287(9), 1132-1141.



Pope C.A. and Dockery D.W. (2006), Health Effects of Fine Particulate Air Pollution: Lines that Connect, Journal of the Air and Waste Management Association, 56, 709-742.

Poschl U. (2005). Atmospheric Aerosol: Composition, transformation, climate and health effects. Reviews: Atmospheric Chemistry, DOI: 10.1002/anie.200501122.

Ramanathan V. and Carmichael G. (2008). Global and Regional Climate Changes Due to Black Carbon. Nat. Geosci. 1: 221–227.

Schiff, K. C. and Weisberg, S. B. (1999). Iron as a reference element for determining trace metal enrichment in Southern California coast shelf sediments. Mar. Environ. Res., 48 (2), 161–176.

Seinfeld and Pandis (1998). Atmospheric Chemistry and Physics: from air pollution to climate. Willey Inter-science, New York.

Seshan B.R.R., Natesan U. and Deepthi K. (2010). Geochemical and statistical approach for evaluation of heavy metal pollution in core sediments in southeast coast of India. Int. J. Environ. Sci. Tech., 7 (2), 291-306, ISSN: 1735-1472.

Sternbeck J., Sjodin A. and Andreasson K. (2002). Metal emissions from road traffic and the influence of resuspension – results from two tunnel studies. Atmospheric Environment, Vol. 36, pp. 4735-4744.

Sutherland, R.A. (2000). Bed sediment-associated trace metals in an urban stream, Oahu, Hawaii. Environ. Geol., 39: 611-37.

Tasic M., Mijic Z., Rajsic S., Zekic A., Perisic M. and Stojic A. (2010). Characteristics and application of receptor models to the atmospheric aerosol research. Air Quality, ISBN: 978-953-307-132-2.

Taylor S.R. (1964). Abundance of chemical elements in the continental crust: a new table. Geochimicu et Cosmochimicn Acta, Vol. 28, pp. 1273 to 1285. Pwgsmon Press Ltd.

Taylor S.R. and McLennan S.M. (1995). The geochemical evolution of the continental crust. Rev. Geophys., 33: 241-265.

Thurstone L.L. (1947). Multiple factor analysis. Chicago: University of Chicago Press.

Udden, J.A. (1896). Dust and Sand Storm in the West: Appleton's Popular Science Monthly, v. XLIX

US EPA (2003). Air toxics website. <http://www.epa.gov/ttn/atw/hlthef/>.

WHO (2000). Guidelines for Air Quality. Expert Task Force meeting held in Geneva, Switzerland, in December 1997.

Wichmann H.E. (2007). Diesel Exhaust Particle. *Inhalation Toxicol.* 19: 241–244.

World Bank Group. (1998). Airborne particulate matter. Pollution prevention and abatement handbook. World Bank Publications, 1999.

Xie S., Zhang J. and Ho Y.S. (2008). Assessment of world aerosol research trends by bibliometric analysis. *Scientometrics*, Vol.77, No.1, 113-130.

Xinwei L., Lijun W., Kai L., Jing H. and Yuxiang Z. (2009). Contamination assessment of copper, lead, zinc, manganese and nickel in street dust of Baoji, NW China. *Journal of Hazardous Materials* 161: 1058–1062.

XRF Newsletter (2009): A newsletter of the IAEA's Laboratories, Seibersdorf Issue No. 18. ISSN 1608–4632.

Zoller W.H. and Gordon G.E. (1970). Instrumental neutron activation analysis of atmospheric pollutants utilizing Ge(Li) Y-ray detectors. *Anal. Chem.*, 42, 257-265.



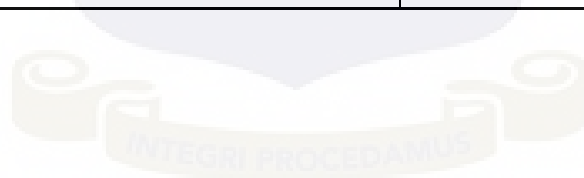
APPENDICES

Table 3.2: Weight of Empty Coarse and Fine filters in microgram ( $\mu\text{g}$ )

Filter ID	Coarse				Fine			
	W1	W2	W3	Average	W1	W2	W3	Average
1	22471	22470	22470	22470	24683	24682	24681	24682
2	22559	22559	22558	22559	24567	24566	24567	24567
3	22429	22428	22429	22429	24442	24441	24441	24441
4	22598	22597	22597	22597	23824	23823	23824	23824
5	22424	22423	22423	22423	23773	23772	23772	23772
6	22380	22379	22379	22379	23612	23613	23612	23612
7	23224	23223	22223	22890	23670	23669	23669	23669
8	22886	22886	22885	22886	24042	24042	22041	23375
9	23124	23124	23123	23124	23998	23999	23998	23998
10	23081	23081	23080	23081	23837	23836	23836	23836
11	23445	23446	23447	23446	23846	23847	23846	23846
12	23178	23179	23178	23178	23878	23877	23877	23877
13	22978	22978	22977	22978	23215	23214	23214	23214
14	23180	23180	23179	23180	23717	23718	23717	23717
15	23139	23139	23138	23139	23965	23965	23964	23965
16	23012	23013	23012	23012	23608	23607	23606	23607
17	22909	22908	22908	22908	23432	23431	23431	23431
18	22799	22778	22778	22785	23613	23612	23612	23612
19	22514	22514	22515	22514	23412	23411	23411	23411
20	23163	23162	23161	23162	23513	23512	23512	23512
21	22160	22159	22159	22159	23357	23357	23356	23357
22	22118	22117	22117	22117	24638	24637	24637	24637
23	22277	22276	22276	22276	25211	25211	25210	25211
24	23089	23088	23088	23088	25736	25735	23735	25069
25	23515	23514	23514	23514	24941	24942	24941	24941

**Table 3.3: Weight of Loaded Coarse and Fine filters in microgram ( $\mu\text{g}$ )**

Filter ID	Coarse				Fine			
	W1	W2	W3	Average	W1	W2	W3	Average
1	22800	22802	22803	22802	25174	25173	25174	25174
2	22903	22904	22904	22904	24900	24899	24900	24900
3	22914	22915	22915	22915	24652	24651	24652	24652
4	22892	22891	22893	22892	24218	24218	24218	24218
5	22846	22846	22846	22846	24308	24306	24308	24307
6	22703	22704	22705	22704	23838	23837	23838	23838
7	23555	23555	23555	23555	23823	23823	23823	23823
8	23618	23618	23618	23618	24041	24040	24041	24041
9	23402	23403	23403	23403	24431	24431	24431	24431
10	23540	23540	23540	23540	24160	24158	24160	24159
11	23896	23897	23897	23897	24526	24526	24526	24526
12	24119	24119	24119	24119	24424	24423	24424	24424
13	23698	23698	23698	23698	23602	23601	23600	23601
14	23574	23573	23574	23574	24034	24033	24034	24034
15	23599	23598	23599	23599	24404	24405	24405	24405
16	23775	23776	23776	23776	24113	24112	24113	24113
17	23494	23495	23495	23495	23823	23822	23823	23823
18	23258	23257	23258	23258	23968	23967	23968	23968
19	23247	23247	23247	23247	23882	23882	23882	23882
20	23693	23694	23694	23694	24793	24793	24793	24793
21	22854	22853	22854	22854	24360	24360	24360	24360
22	22662	22661	22662	22662	24738	24737	24738	24738
23	23055	23055	23055	23055	25742	25741	25742	25742
24	23749	23749	23749	23749	25306	25305	25306	25306
25	23859	23858	23859	23859	25433	25434	25434	25434



**Table 3.4: Average mass in microgram ( $\mu\text{g}$ ) of TSPM collected during sampling**

Filter ID	Date		TSPM Mass ( $\mu\text{g}$ )	
	From	To	Coarse	Fine
1	18/10/12	19/10/12	331	492
2	20/10/12	21/10/12	345	333
3	21/10/12	22/10/12	486	210
4	24/10/12	25/10/12	295	394
5	25/10/12	26/10/12	423	535
6	26/10/12	27/10/12	325	225
7	31/10/12	01/11/12	665	154
8	20/11/12	21/11/12	732	666
9	21/11/12	22/11/12	279	433
10	22/11/12	23/11/12	459	323
11	23/11/12	24/11/12	451	680
12	24/11/12	25/11/12	941	546
13	25/11/12	26/11/12	720	387
14	26/11/12	27/11/12	394	316
15	27/11/12	28/11/12	460	440
16	28/11/12	29/11/12	763	506
17	02/12/12	03/12/12	586	391
18	03/12/12	04/12/12	473	355
19	04/12/12	05/12/12	733	471
20	05/12/12	06/12/12	532	1281
21	06/12/12	07/12/12	694	1003
22	07/12/12	08/12/12	544	100
23	08/12/12	09/12/12	779	531
24	09/12/12	10/12/12	661	237
25	10/12/12	11/12/12	344	492

**Table 3.5: Calculated volume of air sampled in cubic meter (m<sup>3</sup>) during sampling**

Filter ID	Flow Rate (L/min)			Sampling Time (min)	Volume of air sampled	
	Initial	Final	Average		V/L	V/m <sup>3</sup>
1	17	17	17	1440	24480	24
2	17	15	16	1440	23040	23
3	17	15	16	1440	23040	23
4	17	17	17	1440	24480	24
5	17	17	17	1440	24480	24
6	17	15	16	1440	23040	23
7	17	17	17	1440	24480	24
8	17	15	16	1420	22720	23
9	17	15	16	1425	22800	23
10	17	17	17	1425	24225	24
11	17	17	17	1430	24310	24
12	17	17	17	1430	24310	24
13	17	17	17	1430	24310	24
14	17	17	17	1430	24310	24
15	17	17	17	1430	24310	24
16	17	17	17	1430	24310	24
17	17	17	17	1435	24395	24
18	17	17	17	1435	24395	24
19	17	17	17	1435	24395	24
20	17	17	17	1435	24395	24
21	17	17	17	1435	24395	24
22	17	17	17	1435	24395	24
23	17	17	17	1435	24395	24
24	17	17	17	1435	24395	24
25	17	17	17	1435	24395	24

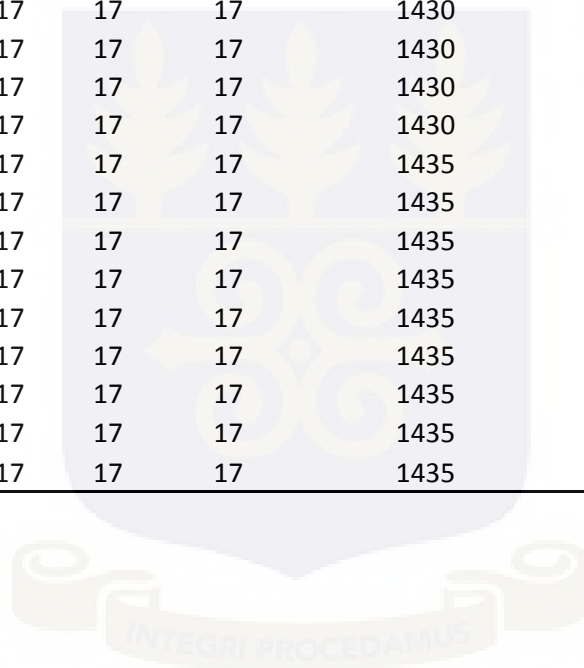


**Table 3.6: Calculated Mass Concentrations ( $\mu\text{g}/\text{m}^3$ ) of TSPM collected during sampling**

Filter ID	Volume of Air Sampled ( $\text{m}^3$ )	TSPM Mass ( $\mu\text{g}$ )		TSPM Conc. ( $\mu\text{g}/\text{m}^3$ )	
		Coarse	Fine	Coarse	Fine
1	24	331	492	13.535	20.084
2	23	345	333	14.974	14.453
3	23	486	210	21.094	9.129
4	24	295	394	12.037	16.108
5	24	423	535	17.266	21.855
6	23	325	225	14.091	9.780
7	24	665	154	27.165	6.277
8	23	732	666	32.233	29.299
9	23	279	433	12.237	18.977
10	24	459	323	18.961	13.333
11	24	451	680	18.538	27.958
12	24	941	546	38.695	22.474
13	24	720	387	29.631	15.906
14	24	394	316	16.207	13.012
15	24	460	440	18.922	18.100
16	24	763	506	31.400	20.801
17	24	586	391	24.035	16.042
18	24	473	355	19.376	14.566
19	24	733	471	30.033	19.294
20	24	532	1281	21.794	52.497
21	24	694	1003	28.462	41.129
22	24	544	100	22.313	4.113
23	24	779	531	31.919	21.767
24	24	661	237	27.082	9.715
25	24	344	492	14.115	20.182

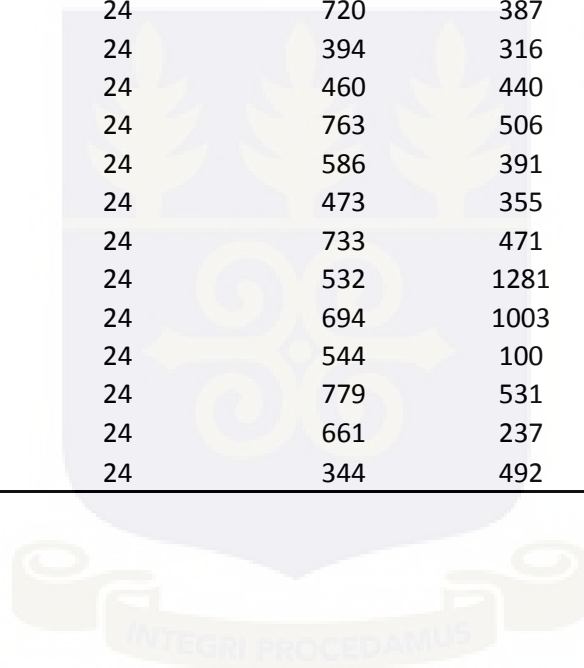


**Table3.8: Net yield in cps/mA of all 28 elements measured by EDXRF in the 20 Coarse Nuclepore filters**

Element	1C	2C	3C	4C	5C	6C	7C	8C	9C	10C	Blank Nuclepore	Blank Mylar	STD ALL	STD Conc. (µg/cm <sup>2</sup> )
Na	0.041	0.034	0.081	0.053	0.048	0.058	0.039	0.050	0.066	0.051	0.000	0.017	1.108	21.912
Mg	0.057	0.062	0.088	0.064	0.059	0.073	0.055	0.081	0.069	0.052	0.000	0.028	3.078	20.054
Al	0.257	0.157	0.236	0.145	0.244	0.217	0.202	0.366	0.193	0.482	0.000	0.035	16.142	46.900
Si	0.583	0.341	0.494	0.348	0.637	0.484	0.527	0.948	0.448	1.118	0.000	0.023	15.389	27.332
S	0.320	0.387	0.557	0.425	0.432	0.532	0.408	0.803	0.407	0.543	0.000	0.040	22.720	15.300
Cl	5.444	6.188	9.109	5.785	5.932	7.017	4.657	6.584	6.007	6.506	0.124	0.031	70.357	33.788
K	0.827	0.891	1.181	0.891	1.113	0.809	0.722	1.312	0.660	0.993	0.000	0.000	85.522	23.130
Ca	3.254	2.201	3.279	2.169	2.869	4.565	2.182	6.057	2.492	5.810	0.000	7.227	159.188	27.206
Ti	0.142	0.077	0.112	0.070	0.138	0.118	0.106	0.226	0.114	0.281	0.000	0.007	142.712	44.300
V	0.009	0.007	0.003	0.008	0.005	0.008	0.013	0.013	0.012	0.013	0.000	0.005	177.384	45.700
Cr	0.069	0.053	0.057	0.062	0.061	0.065	0.049	0.056	0.068	0.070	0.000	0.020	247.038	45.300
Mn	0.082	0.055	0.067	0.065	0.096	0.056	0.064	0.099	0.055	0.089	0.000	0.058	156.205	49.600
Fe	2.049	1.105	1.858	0.987	2.078	1.630	1.514	3.244	1.399	3.830	0.104	0.128	189.839	49.000
Ni	0.002	0.008	0.008	<LLD	0.011	0.009	0.008	0.009	0.004	0.010	0.000	0.004	254.251	44.300
Cu	0.068	0.065	0.073	0.072	0.078	0.082	0.064	0.082	0.076	0.075	0.000	0.058	280.021	44.600
Zn	0.196	0.202	0.219	0.215	0.226	0.236	0.204	0.268	0.195	0.229	0.000	0.478	118.205	16.572
Br	0.068	0.089	0.133	0.066	0.087	0.091	0.077	0.107	0.063	0.069	0.000	0.006	117.488	18.736
Rb	<LLD	0.006	<LLD	0.009	<LLD	0.002	<LLD	0.009	0.002	0.008	0.000	0.006	144.809	19.439
Sr	0.080	0.070	0.070	0.069	0.080	0.087	0.075	0.094	0.080	0.087	0.000	0.037	106.625	33.759
Zr	0.014	0.011	0.023	0.001	0.015	0.012	0.017	0.013	0.010	0.015	0.000	0.004	152.300	34.200
Mo	0.020	0.029	0.034	0.028	0.035	0.029	0.021	0.025	0.028	0.023	0.000	0.028	167.236	34.859
Pd	<LLD	0.027	0.009	0.008	0.004	0.006	0.016	0.018	0.020	0.016	0.000	0.023	175.470	45.600
Cd	0.026	0.034	0.010	0.013	0.021	0.026	0.028	0.005	0.019	0.020	0.000	0.020	136.731	30.839
Sn	0.052	0.053	0.083	0.051	0.050	0.032	0.040	0.034	0.086	0.042	0.000	0.064	116.981	43.900
Cs	0.028	0.038	0.041	0.043	0.041	0.048	0.031	0.033	0.037	0.044	0.000	0.033	26.636	31.164
Ba	0.032	0.057	0.060	0.048	0.047	0.055	0.049	0.045	0.047	0.040	0.000	0.033	29.538	35.637
Pt	0.061	0.050	0.059	0.059	0.067	0.063	0.060	0.052	0.064	0.052	0.000	0.054	128.136	44.000
Pb	0.038	0.021	0.034	0.018	0.038	0.028	0.024	0.030	0.029	0.028	0.000	0.026	147.474	51.300



**Table 3.8: Continued.**

Element	11C	12C	13C	14C	15C	16C	17C	18C	19C	20C	Blank Nuclepore	Blank Mylar	STD ALL	STD Conc. (µg/cm <sup>2</sup> )
Na	0.036	0.054	0.052	0.065	0.046	0.050	0.040	0.054	0.061	0.043	0.000	0.017	1.108	21.912
Mg	0.066	0.076	0.057	0.063	0.056	0.088	0.056	0.053	0.070	0.050	0.000	0.028	3.078	20.054
Al	0.537	0.749	0.659	0.213	0.380	0.529	0.553	0.277	0.742	0.108	0.000	0.035	16.142	46.900
Si	1.289	1.866	1.589	0.616	0.987	1.495	1.638	0.711	1.667	0.258	0.000	0.023	15.389	27.332
S	0.653	0.731	0.551	0.327	0.379	0.682	0.599	0.367	0.555	0.227	0.000	0.040	22.720	15.300
Cl	6.831	8.022	8.545	6.364	5.877	9.215	5.967	5.011	10.133	3.071	0.124	0.031	70.357	33.788
K	1.138	1.548	1.640	0.778	0.898	1.418	1.403	1.245	1.768	0.646	0.000	0.000	85.522	23.130
Ca	5.871	9.121	5.421	2.620	4.818	5.784	6.496	4.133	7.233	1.701	0.000	7.227	159.188	27.206
Ti	0.304	0.475	0.379	0.108	0.200	0.312	0.354	0.156	0.415	0.051	0.000	0.007	142.712	44.300
V	0.010	0.015	0.020	0.005	0.006	0.007	0.027	0.011	0.017	0.005	0.000	0.005	177.384	45.700
Cr	0.051	0.075	0.070	0.050	0.064	0.071	0.061	0.064	0.064	0.068	0.000	0.020	247.038	45.300
Mn	0.092	0.102	0.102	0.098	0.119	0.072	0.101	0.052	0.102	0.036	0.000	0.058	156.205	49.600
Fe	4.279	6.195	5.539	1.741	3.047	3.997	5.041	2.379	5.767	0.733	0.104	0.128	189.839	49.000
Ni	0.014	0.007	0.007	0.009	0.013	0.009	0.009	0.006	0.006	0.009	0.000	0.004	254.251	44.300
Cu	0.070	0.072	0.081	0.072	0.067	0.078	0.059	0.065	0.074	0.057	0.000	0.058	280.021	44.600
Zn	0.243	0.248	0.253	0.212	0.200	0.237	0.239	0.207	0.253	0.175	0.000	0.478	118.205	16.572
Br	0.081	0.109	0.100	0.066	0.056	0.156	0.054	0.048	0.110	0.036	0.000	0.006	117.488	18.736
Rb	0.002	0.004	0.010	0.011	0.006	0.005	0.007	<LLD	0.008	0.004	0.000	0.006	144.809	19.439
Sr	0.080	0.098	0.076	0.076	0.081	0.115	0.082	0.070	0.088	0.067	0.000	0.037	106.625	33.759
Zr	0.014	0.019	0.014	0.003	0.008	0.021	0.018	0.006	0.022	0.007	0.000	0.004	152.300	34.200
Mo	0.033	0.045	0.024	0.028	0.031	0.023	0.044	0.026	0.014	0.036	0.000	0.028	167.236	34.859
Pd	<LLD	0.006	0.011	<LLD	0.016	0.007	0.025	0.014	0.030	0.022	0.000	0.023	175.470	45.600
Cd	0.029	0.011	0.020	0.013	0.022	0.010	0.015	0.010	0.027	0.015	0.000	0.020	136.731	30.839
Sn	0.035	0.053	0.079	0.078	0.074	0.061	0.045	0.071	0.051	0.030	0.000	0.064	116.981	43.900
Cs	0.031	0.039	0.040	0.038	0.048	0.023	0.036	0.040	0.031	0.030	0.000	0.033	26.636	31.164
Ba	0.035	0.046	0.048	0.065	0.033	0.052	0.056	0.034	0.053	0.036	0.000	0.033	29.538	35.637
Pt	0.057	0.055	0.059	0.045	0.061	0.046	0.054	0.043	0.061	0.052	0.000	0.054	128.136	44.000
Pb	0.030	0.035	0.025	0.024	0.030	0.032	0.025	0.025	0.025	0.016	0.000	0.026	147.474	51.300

**Table 3.9: Calculated values of elemental concentrations ( $\mu\text{g}/\text{m}^3$ ) of all 28 elements measured by EDXRF**

Element	Filter ID									
	1C	2C	3C	4C	5C	6C	7C	8C	9C	10C
Na	0.692	0.444	1.026	0.632	0.572	0.653	0.465	0.663	0.845	0.614
Mg	0.315	0.265	0.365	0.250	0.230	0.269	0.215	0.352	0.289	0.205
Al	0.629	0.298	0.433	0.251	0.422	0.354	0.349	0.703	0.358	0.842
Si	0.872	0.395	0.554	0.367	0.672	0.483	0.556	1.113	0.508	1.193
S	0.181	0.170	0.237	0.170	0.173	0.201	0.163	0.358	0.175	0.220
Cl	2.149	1.896	2.722	1.614	1.656	1.856	1.292	2.049	1.801	1.839
K	0.188	0.157	0.201	0.143	0.179	0.123	0.116	0.234	0.114	0.161
Ca	0.490	0.256	0.370	0.230	0.305	0.458	0.232	0.716	0.284	0.624
Ti	0.037	0.016	0.022	0.013	0.025	0.021	0.020	0.046	0.023	0.052
V	0.002	0.001	0.000	0.001	0.001	0.001	0.002	0.002	0.002	0.002
Cr	0.011	0.006	0.007	0.007	0.007	0.007	0.005	0.007	0.008	0.008
Mn	0.022	0.011	0.013	0.012	0.018	0.010	0.012	0.021	0.011	0.017
Fe	0.422	0.168	0.286	0.135	0.303	0.221	0.216	0.535	0.213	0.577
Ni	0.000	0.001	0.001	<LLD	0.001	0.001	0.001	0.001	0.000	0.001
Cu	0.009	0.007	0.007	0.007	0.007	0.007	0.006	0.009	0.008	0.007
Zn	0.023	0.019	0.019	0.018	0.019	0.019	0.017	0.025	0.017	0.019
Br	0.009	0.009	0.013	0.006	0.008	0.008	0.007	0.011	0.006	0.007
Rb	<LLD	0.001	<LLD	0.001	<LLD	0.000	<LLD	0.001	0.000	0.001
Sr	0.021	0.014	0.014	0.013	0.015	0.015	0.014	0.020	0.016	0.017
Zr	0.003	0.002	0.003	0.000	0.002	0.002	0.002	0.002	0.001	0.002
Mo	0.004	0.004	0.004	0.003	0.004	0.003	0.003	0.003	0.004	0.003
Pd	<LLD	0.005	0.001	0.001	0.001	0.001	0.002	0.003	0.003	0.002
Cd	0.005	0.005	0.001	0.002	0.003	0.003	0.004	0.001	0.003	0.003
Sn	0.016	0.013	0.020	0.011	0.011	0.007	0.009	0.008	0.021	0.009
Cs	0.028	0.029	0.030	0.030	0.029	0.032	0.022	0.026	0.028	0.031
Ba	0.032	0.045	0.046	0.034	0.034	0.037	0.035	0.036	0.036	0.029
Pt	0.018	0.011	0.013	0.012	0.014	0.012	0.012	0.012	0.014	0.011
Pb	0.011	0.005	0.007	0.004	0.008	0.005	0.005	0.007	0.006	0.006

**Table 3.9: Continued.**

Element	Filter ID									
	11C	12C	13C	14C	15C	16C	17C	18C	19C	20C
Na	0.432	0.648	0.624	0.780	0.552	0.600	0.478	0.646	0.730	0.514
Mg	0.259	0.299	0.224	0.248	0.220	0.346	0.219	0.208	0.274	0.196
Al	0.934	1.303	1.147	0.371	0.661	0.921	0.959	0.480	1.287	0.187
Si	1.370	1.984	1.689	0.655	1.049	1.589	1.735	0.753	1.766	0.273
S	0.263	0.295	0.222	0.132	0.153	0.275	0.241	0.147	0.223	0.091
Cl	1.926	2.268	2.418	1.792	1.652	2.610	1.672	1.398	2.864	0.843
K	0.184	0.250	0.265	0.126	0.145	0.229	0.226	0.201	0.285	0.104
Ca	0.628	0.976	0.580	0.280	0.515	0.619	0.693	0.441	0.771	0.181
Ti	0.056	0.088	0.070	0.020	0.037	0.058	0.065	0.029	0.077	0.009
V	0.002	0.002	0.003	0.001	0.001	0.001	0.004	0.002	0.003	0.001
Cr	0.006	0.008	0.008	0.005	0.007	0.008	0.007	0.007	0.007	0.007
Mn	0.017	0.019	0.019	0.019	0.023	0.014	0.019	0.010	0.019	0.007
Fe	0.644	0.940	0.839	0.253	0.454	0.601	0.759	0.350	0.871	0.097
Ni	0.001	0.001	0.001	0.001	0.001	0.001	0.001	0.001	0.001	0.001
Cu	0.007	0.007	0.008	0.007	0.006	0.007	0.006	0.006	0.007	0.005
Zn	0.020	0.021	0.021	0.018	0.017	0.020	0.020	0.017	0.021	0.015
Br	0.008	0.010	0.010	0.006	0.005	0.015	0.005	0.005	0.010	0.003
Rb	0.000	0.000	0.001	0.001	0.000	0.000	0.001	<LLD	0.001	0.000
Sr	0.015	0.019	0.014	0.014	0.015	0.022	0.015	0.013	0.017	0.013
Zr	0.002	0.003	0.002	0.000	0.001	0.003	0.002	0.001	0.003	0.001
Mo	0.004	0.006	0.003	0.003	0.004	0.003	0.005	0.003	0.002	0.004
Pd	<LLD	0.001	0.002	<LLD	0.002	0.001	0.004	0.002	0.005	0.003
Cd	0.004	0.001	0.003	0.002	0.003	0.001	0.002	0.001	0.004	0.002
Sn	0.008	0.012	0.018	0.018	0.017	0.014	0.010	0.016	0.011	0.007
Cs	0.022	0.027	0.028	0.027	0.034	0.016	0.025	0.028	0.022	0.021
Ba	0.025	0.033	0.035	0.047	0.024	0.038	0.040	0.024	0.038	0.026
Pt	0.012	0.011	0.012	0.009	0.013	0.009	0.011	0.009	0.012	0.011
Pb	0.006	0.007	0.005	0.005	0.006	0.007	0.005	0.005	0.005	0.003

**Table 3.10: Range of elemental abundances in the CPM ( $\mu\text{g}/\text{m}^3$ ) from the Abuesi area measured by EDXRF with their respective Enrichment Factor (EF) values**

Element	Range	Mean	Standard Deviation	EF
Na	0.432 - 1.026	0.631	0.143	3.386
Mg	0.196 - 0.365	0.262	0.051	1.427
Al	0.187 - 1.303	0.644	0.351	0.992
Si	0.273 - 1.984	0.979	0.543	0.441
S	0.091 - 0.358	0.205	0.062	0.010
Cl	0.843 - 2.864	1.916	0.493	0.187
K	0.104 - 0.285	0.181	0.054	1.101
Ca	0.181 - 0.976	0.482	0.216	1.473
Ti	0.009 - 0.088	0.039	0.023	0.872
V	0.001 - 0.004	0.002	0.001	0.000
Cr	0.005 - 0.011	0.007	0.001	0.001
Mn	0.007 - 0.022	0.016	0.005	0.000
Fe	0.097 - 0.940	0.444	0.263	1.000
Ni	0.000 - 0.001	0.001	0.000	0.000
Cu	0.005 - 0.009	0.007	0.001	0.002
Zn	0.015 - 0.025	0.019	0.002	0.003
Br	0.003 - 0.015	0.008	0.003	0.041
Rb	0.000 - 0.001	0.001	0.000	0.000
Sr	0.013 - 0.022	0.016	0.003	0.001
Zr	0.000 - 0.003	0.002	0.001	0.000
Mo	0.002 - 0.006	0.004	0.001	0.031
Pd	0.001 - 0.005	0.002	0.001	—
Cd	0.001 - 0.005	0.003	0.001	0.166
Sn	0.007 - 0.021	0.013	0.004	0.081
Cs	0.016 - 0.034	0.027	0.004	0.112
Ba	0.024 - 0.047	0.035	0.007	0.001
Pt	0.009 - 0.018	0.012	0.002	—
Pb	0.003 - 0.011	0.006	0.002	0.006